The Thesis Committee for Benjamin James Spisak
Certifies that this is the approved version of the following thesis:

Using Nanoparticle Stabilized Foam to Achieve Wellbore Stability in Shales

APPROVED BY
SUPERVISING COMMITTEE:

Supervisor: _____
Mukul M. Sharma

Co-supervisor: _____
Martin E. Chenevert

Using Nanoparticle Stabilized Foam to Achieve Wellbore Stability in Shales

by

Benjamin James Spisak, BS

Thesis

Presented to the Faculty of the Graduate School of

The University of Texas at Austin

in Partial Fulfillment

of the Requirements

for the Degree of

Master of Science in Engineering

The University of Texas at Austin

August 2011

Dedication

To my family, friends, colleagues, and God.

Acknowledgements

I would like to thank my supervisors Dr. Mukul M. Sharma and Dr. Martin E. Chenevert for their support and dedication to the completion of the work presented in this thesis. Their efforts to help me improve on my work ethic, communication skills, and technical skills as an engineer are invaluable and will be practiced for the rest of my career.

This work would not have been completed without the aid and support of Glen Baum and Gary Miscoe. The incredible efforts given by these men through countless calibrations, troubleshooting equipment, and supplying equipment and expertise was truly vital to the completion of these experiments. The support I have received by these men is much appreciated.

I would like to thank Dr. Holder and Harry Linnemeyer for aiding in the troubleshooting of the experimental equipment. I am thankful for Dr. Holder's efforts to help troubleshoot the data acquisition part of the experimental setup when time was of the essence. Harry Linnemeyer has been a great help by working with me through ideas for the experiment to advising in methods to reach the end product presented in this thesis. Harry was also helpful in the acquisition of equipment to make sure the experiments ran smoothly.

I would like to thank my research group which included Dr. Rui Zhang, Dr. Jihua Cai, and Chang Min Jung. Many times we worked together to run experiments and gather data. They also helped keep me going when frustrations set in and were there to help when the work load was very large. I would also like to thank Jin Kyung Lee and Frankie Hart for their administrative support during this work. They helped keep me organized throughout my time in graduate school.

I would like to thank those who provided me with financial support during my graduate school work. I would like to thank Yates Petroleum Corporation and British Petroleum Incorporated for the fellowships they provided. I would like to thank RPSEA for the contract that supported me during my thesis work.

The support of my family and friends in this thesis helped keep me sane and provided motivation to succeed in my graduate school work. Without their support this work would not have been possible. I would like to thank my parents for believing in me and supporting me both financially and as their son through all of my endeavors.

Lastly, I would like to thank my Lord and Savior, Jesus Christ, for providing me with the opportunities to succeed and calling me to the purpose set out ahead.

Abstract

Using Nanoparticle Stabilized Foams to Achieve Wellbore Stability in Shales

Benjamin James Spisak, M.S.E.

The University of Texas at Austin, 2011

Supervisors: Mukul M. Sharma and Martin E. Chenevert

Foams have been used successfully in the industry for both drilling and fracturing. These foams usually consist of both an aqueous liquid phase and a gas phase; air, nitrogen, and/or CO_2 are the most common. Due to the aqueous liquid component in the foam, drilling and fracturing in shale formations can cause swelling and collapsing of the rock through formation invasion. Sensoy et al.(2009) has shown that the addition of nanoparticle dispersions to water based fluids reduces the amount of water invading the shale and has been used as a kickoff point for this research. Results presented in this thesis show that the addition of nanoparticles to foams enhances the performance of these fluids by reducing their invasion into shale. The use of foams allows for a low concentration of nanoparticles making this technology much more economically feasible for field testing and use.

Table of Contents

List of Tables

List of Figures

CHAPTER 1: BACKGROUND

Foams are very unique and complex fluids. To gain a better understanding of the nature of foams, a brief literature review has been undertaken. Researchers studying foam rheological properties have been in disagreement on the classification of foam. While most agree that foam behaves as a pseudoplastic or Bingham plastic fluid, there is disagreement about which model best predicts flow behavior. The dominating model is the Herschel-Buckley model, but there have also been studies showing foam rheology closely following a power law model. The flow performance differences between studies can likely be linked to the method of foam generation and stabilization (Saintpere et al., 1999). The very nature of foams, consisting of bubbles breaking and reforming, as well as gas fluid being compressed, restricts steady state flow from truly being reached.

The key defining parameter that classifies foam is its quality. Quality is the volume percentage of gas in the foam's total volume. It is represented by the following equation:

$$\Gamma = \frac{100V_g}{V_g + V_l}$$

Γ is the foam quality (%)

V_g is the volume of gas

V_l is the volume of liquid

Therefore, a higher percentage of gas drives the quality of the foam higher.

Even though there has been disagreement in the general model used to predict rheological properties, there have been some consistent characteristics viewed while

studying foam's rheology. The apparent viscosity of foam has been shown to be dependent on five main foam properties (Caiweizel, 1987):

- Foam quality increases, apparent viscosity has been shown to increase, even exponentially at high values of quality.
- As temperature increases, the apparent viscosity of the foam decreases.
- Apparent viscosity increases as bubble-size increases.
- As pressure increases, the apparent viscosity of the foam increases until a critical pressure has been reached, and then remains relatively constant.
- The addition of stabilizers, such as polymer or nanoparticles, increases the apparent viscosity of the foam.

The yield point or yield stress of the foam shows a similar dependency on the above five parameters.

1.1 DRILLING

Drilling with foam is often used when an underbalanced drilling technique is applied. Results from the field have shown distinct economic advantages when foam drilling has been correctly applied. Underbalanced drilling can result in higher drilling rates and minimize formation damage. Underbalanced drilling is advantageous when drilling through fractured layers, unconsolidated sands, tight formations, and low pressure reservoirs. When employed correctly to the previously noted situations, four main advantages can be realized (Negrao et al., 1997):

- Minimal damage to sensitive hydrocarbon formations

- Faster evaluation of cuttings at the rig floor for hydrocarbon determination
- Prevention of loss circulation into the formation
- Increased rates of penetration with the drill bit

Economic enhancement can only be obtained if the correct situations are present. There are some disadvantages to using this technique as well, like the need for extra equipment at the surface. For example, extra separation and pumping equipment are necessary so as to recover the foam. This can lead to logistical issues when space is limited, such as on offshore platforms or remote locations where getting equipment to the well site is difficult.

One of the more dangerous situations is the use of this technique on a high pressure well. Large, high pressure kicks can move up the annular space at very high rates, so using underbalanced foam drilling is not advisable.

1.2 FRACTURING

The other application of this research is the use of foams for fracturing. Fracturing occurs when the wellbore pressure is increased past the pore and overburden pressures in the formation. One difficulty when using foams is calculating the friction loss, wellhead pressure, and the resulting density and carrying capabilities during treatment (Caiwiezel et al., 1987). Simulators have been used, so far, to predict these parameters and have been shown to work within a range of error, but work still needs to be performed to create more robust and accurate simulators.

Despite this margin of error, foams still can be used with great success. Foams have high sand or propant carrying capability, low fluid loss, low hydrostatic head, low-friction pressure drops, quick fluid recovery, low formation damage, and lower reduction of fracture conductivity due to fluid ingredients, such as clays (Caiwiezel et al., 1987).

CHAPTER 2: INTRODUCTION

2.1 INTRODUCTION TO THE TECHNOLOGY

In the past, shales have consisted of 75% of the footage drilled throughout the world (Steiger, 1992). It has become even more important in the U.S. with the exploration and production of large shale-gas plays, such as Marcellus and Haynesville. It has also been noted that shale is responsible for 90% of wellbore stability problems such as hole-collapse and stuck-pipe. When drilling with a water based mud (WBM), water enters in through nano-scale size pores and produces swelling within the shale. It has been shown that the pores of most shale have diameters between 10nm and 30nm (Sensoy et al., 2009).

Previous work proposed using nanoparticles (NP's) to build a bridge plug to the pores in the shale to inhibit water flow. Studies by Abrams (1977) and Suri and Sharma (2004) have concluded that the particles be no smaller than one third of the pore throat diameter, hence particle size should be between 3nm and 10nm. A study by Sensoy et al. (2009) used conventional WBM's with an addition of NP's to achieve reduction in permeating water through the shale. This leads to a reduction in the amount of water chemically reacting with the shale, and thus an increase in wellbore stability. Complete plugging has been seen in several instances of increased nanoparticle concentration in the mud. The standard amount of NP's added to achieve wellbore stability was shown to be 10% by weight.

The addition of NP's to foam increases the stability of foam as well as bridges pore throats of shale. Surfactants are employed as the foaming agent and helps stabilize the foam along with the NP's. Research by Espinosa et al. (2009) have shown that stable supercritical CO_2 foams with de-ionized water have been produced with only 0.05% by weight and 4% by weight NP's as a foaming agent. NaCl brine with supercritical CO_2 have been produced with a 0.5% by weight addition of NP's.

NP stabilized foams have been shown to be have definite advantages over a purely surfactant stabilized foam. When adding solid particles to foam, a "Pickering Emulsion" is formed. It has long been known that solids can stabilize emulsions through "steric" stabilization (Tambe and Sharma, 1993). The solid particles act similarly to stabilize foams. They prevent the rupture of the thin fluid films separating the gas bubbles. Micro-scale investigations are still ongoing to explain the governing mechanism for increases in stability due to the addition of NP's in emulsions and foams.

Foam has the distinct advantage that desorption of the NP's at the liquid phase of the foam does not cause the NP's at the gas liquid interface to also desorb, as is the case with surfactants. In addition, NP's can withstand high temperatures within the well; and, being silica, can be considered inert. Espinosa et al (2009) have also shown these NP stabilized foams can perform well in highly saline environments. There have been some drawbacks to this NP and mud research. The surface charges of the different NP's have shown to have large effects on the rheology of the water based muds. A thickening has been seen as well as either a drop or increase in pH has also been observed. These effects have been erratic and difficult to predict. A major drawback to this technique is the cost

of adding NP's into the mud. 10% by weight incurs a high cost in purchasing the amount of NP's for field use.

Just like earlier cases, there are also drawbacks when using NP's to stabilize foam. A resistance to flow has been seen that is 2 to 18 times larger when NP's were added to the liquid phase than that of the foams without any stabilizers added (Espinosa et al 2009). This makes calculation of friction loss in the wellbore even more difficult, but can be possibly reconciled with further research on the rheology of these foams.

The methods used to calculate permeability in this work have the assumption that liquid single phase flow is occurring through the shale. The entrance pressure for gas and liquid has been reviewed in order to confirm this assumption. The equation that governs the entrance pressure is the capillary pressure equation:

$$P_c = \frac{2\sigma \cos\theta}{r} \tag{2.1}$$

Pc is the capillary pressure (psi)

σ is the interfacial tension (dynes/cm)

θ is the contact angle (degrees)

r is the radius of the pore throats (m)

AL-Bazali et al. (2009) have measured the entrance pressure using several non-wetting fluids on different shale. The entrance pressure of nitrogen gas entering water wet Pierre Shale, C1 Shale, and Arco-China shale were measured at 630 psi, 700 psi, and 950 psi respectively. These pressures are a direct reflection of nitrogen's interfacial

tension of 72 dynes/cm. Therefore the assumption that nitrogen gas will not enter our shale cores is a safe assumption.

2.1 Development of Methodology

Developing the procedure for the experiments has been based both on past work and trial and error. Similar experiments have been run using drilling WBM's to perform pressure penetration tests and show reduction of permeability generated from different additives including NP's. Techniques have been borrowed from those experiments (Sensoy et al 2009).

The base fluids used to generate our foam have been chosen to be nitrogen and water. Both of these fluids are readily available for field use. Also, they are safe for use, especially at high pressures, in a lab setting. The use of nitrogen as the gaseous phase in foam also removes the risk of flammable gases entering downhole environments. CO_2 is not included because pH would need to be monitored for the production of carbonic acid. Therefore, both nitrogen and water are non-corrosive, non-flammable, and environmentally friendly fluids for both use down-hole as well as their transportation to the well-site.

The test cell used to perform the pressure penetration tests has a maximum pressure of ~400 psi before the o-rings begin to leak. It has been standard practice for both safety and equipment restrictions to run the tests at an upstream pressure of 300psi. This pressure restriction of the test cell also dictates the pressure at which foam can be made and tested. For all tests performed, the foam pressure has been restricted to 300psi

for foam generation. At higher pressures, higher quality foams can be produced, and it would be interesting to study the effects of NP's in such foam.

McLennan et al., (1997) as well as initial experimentation, has shown that 70% quality foam is the ideal mixture for 300psi. Quality is defined as the volumetric percent of gas in the foam, so 70% quality is identical to 70% gas in the foam. McLennan et al., (1997) have indicated that the range of quality foam for both fracturing and drilling is between 70% and 85%. Initial experimentation with the flow loop has indicated that very stable foam is produced at ~70% quality. Below 70% quality two-phase flow can be seen. Above 70% quality large pockets of gas develop reducing the homogeneity of the foam. For the pressure penetration tests, direct contact between the shale and water will rapidly increase the downstream pressure, and result in a higher representative permeability for the foam.

Espinosa et al. (2009) have described the advantages to using different NP's in their work with supercritical CO_2 foam. Along with their recommendation, we have chosen to use surface modified NP's. The surfaces of these NP's have been coated with a polymer to reduce the effect of the surface charges that these NP's inherently develop. Sensoy et al. (2009) indicated that untreated NP's have a substantial effect on the pH and thickness of water-based muds in which they are injected. To avoid these effects, the surface treated NP's have been chosen due to their neutral pH and the decrease in their surface charges.

2.2 SCOPE OF WORK

We have selected several key characteristics to measure through the generation of foam and the pressure penetration test. In order to measure the quantitative effects of the addition of NP's to the foam, we will measure viscosity, half-life, and permeability of the foam through a sample of shale.

The pressure penetration tests will measure the permeability to study the effects of differing concentrations of NP's in the foam. The concentrations to be measured are 5%, 2%, and 1%.

Tests measuring the permeability of two different shale cores have been run using the aforementioned NP concentrations. The tests performed use samples from two types of shale cores; an Atoka shale and a typical Texas gas shale (TGS). Atoka shale is not known as a reservoir rock and a good simulation for the effects while drilling. The TGS is a reservoir rock and suggests the possible use of NP's in foam for both drilling and fracturing.

Lastly, the Foam Decay Time will be measured using a graduated cylinder filled with 100 mL of foam. A stopwatch will be used to measure the amount of time for the two phases to completely separate. Foam at a rig site needs to be broken down because the pits are not large enough to handle the increase in volume that occurs when the gas expands exiting from the well.

2.3 SHALE PROPERTIES

To show validity of our experiments, proper shale has been selected. Shale from formations commonly drilled through or reservoir shale from formations that is both drilled through and/or fractured is acceptable. Special procedures to preserve these cores have been performed to eliminate the changing of the properties of the shale. Shale has very high clay content and is therefore very water sensitive. Exposure to the atmosphere for any extended period of time will dry out and crack the shale. Pore size is dependent on the amount of water inside the shale, or its water activity (a_w). So cores used in the experiments, presented below, have been specially sealed and the water activity has been precisely controlled. Below are the inherent properties of the shale used.

2.3.1 Atoka Shale

Atoka shale is not a reservoir rock and is water wet with an inherent water activity of approximately 0.72. Atoka is considered relatively "hard" shale, meaning it is not easy broken or cracked compared to many other types of shale. The main composition of Atoka shale, shown in Table 2.1, is quartz and feldspar. Quartz and feldspar are known to be "hard" materials. In order to determine the water activity of the Atoka core, samples of the shale core were put in several different water activity desiccators and the weight change percentages were recorded. This procedure is described by Sensoy et al. (2009). The results for Atoka were as follows in Figure 2.1(Sensoy et al. 2009):

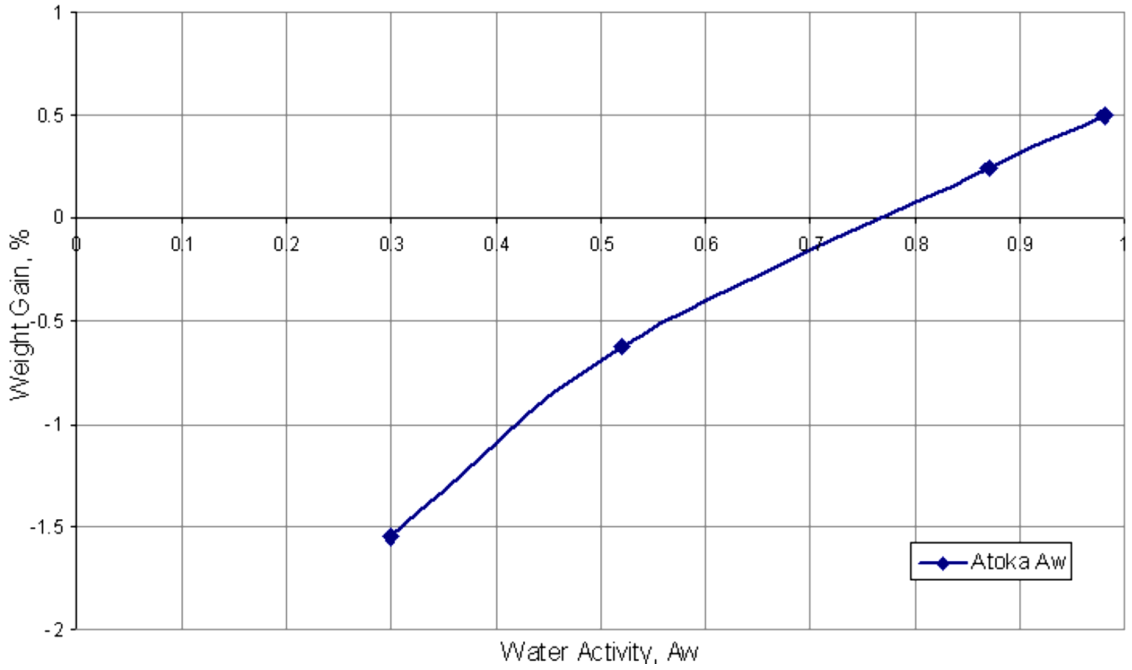

Figure 2.1 Adsortion Isotherm for Atoka Shale

The following table shows the mineralogical composition of Atoka shale using X-Ray Diffraction:

X-Ray Diffraction	Wt %
Quartz	52
Feldspar	15
Total Clay	33
Kaolinite	32
Chlorite	7
Illite	31
Smectite	19
Mixed Layer	11

Table 2.1 X-ray Diffraction of Atoka

2.3.2 TGS

The gas shale core used is from a Texas gas shale (TGS) reservoir. Unlike Atoka shale, the TGS used is more brittle and easily damaged. There is a high content of calcite

and dolomite in the shale which lends the rock to being brittle and easily cracked. The same procedure used to find the native water activity, described above, was applied to the TGS. The main difference between TGS and Atoka is that TGS is oil-wet gas. Figure 2.2 shows the same curve as presented above for the gas-shale.

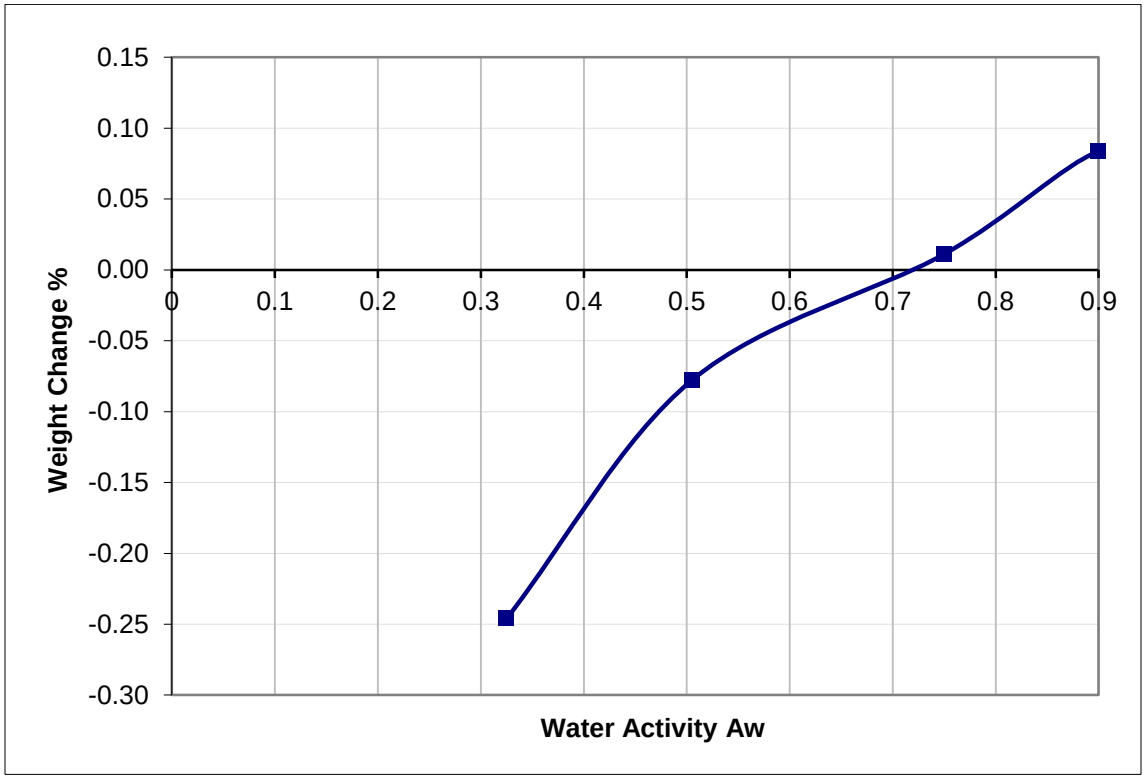

Figure 2.2 Adsorption Isotherm for TGS

Table 2.2 shows the mineralogic composition of the gas-shale:

X-Ray Diffraction	Wt %
Quartz	11
Feldspar	1
Plag.	1
Pyrite	1
Kaolinite	Trace
Chlorite	Trace
Illite	4
Calcite	58
Dolomite	23

Table 2.2 X-ray Diffraction of TGS

As well, this core is an actual reservoir core so, unlike Atoka, there are other fluids initially taking up the pore space. A crushed core analysis was performed by a professional oilfield service company and the rock properties from that test are shown in Table 2.3 below.

A-R Bulk Density, gm/cc	A-R Grain Density, gms/cc	A-R Water Saturation, % of PV	A-R Oil Saturation, % of PV	A-R Gas Saturation, % of PV	A-R Gas Filled Porosity, % of BV
2.55	2.6	42.1	20.5	37.4	1.8

Table 2.3 Crushed Core Analysis of TGS

CHAPTER 3: EQUIPMENT, PROCEDURE, AND CALCULATIONS

The following chapter describes the experimental setup, the procedures performed, and the calculations used. The equipment description will include ranges and an accurate description of the pieces of equipment. Following the equipment description, a detailed procedure for foam generation and a pressure penetration test will be explained. Lastly, the calculations used to generate usable results will be detailed.

3.1 EQUIPMENT

The following is a flow diagram of both the foam flow loop and pressure penetration set up.

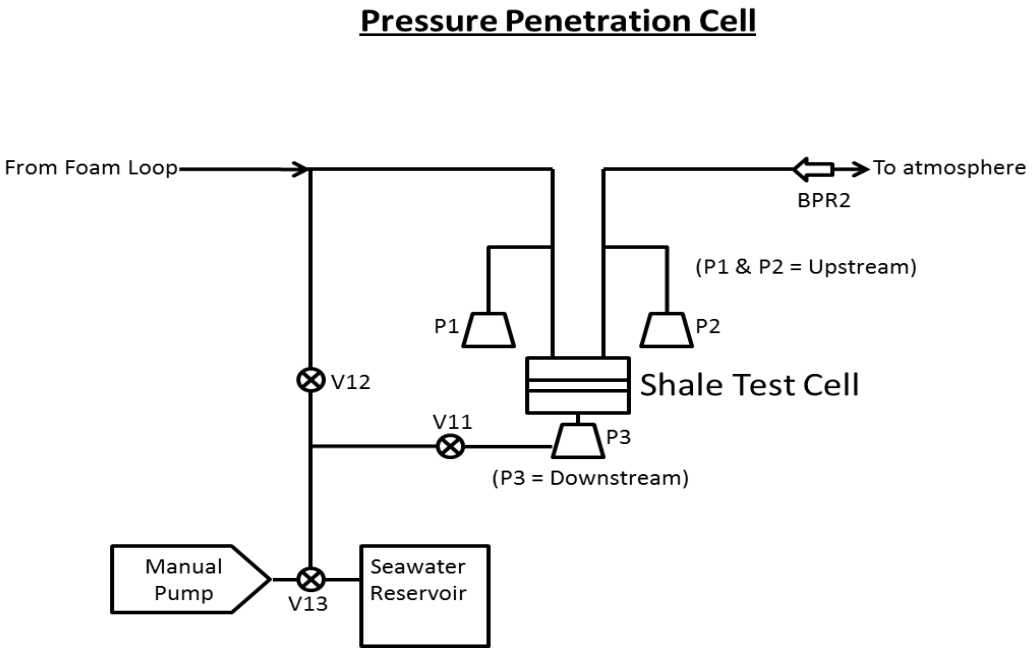

Figure 3.1 Flow Diagram of Pressure Penetration Cell

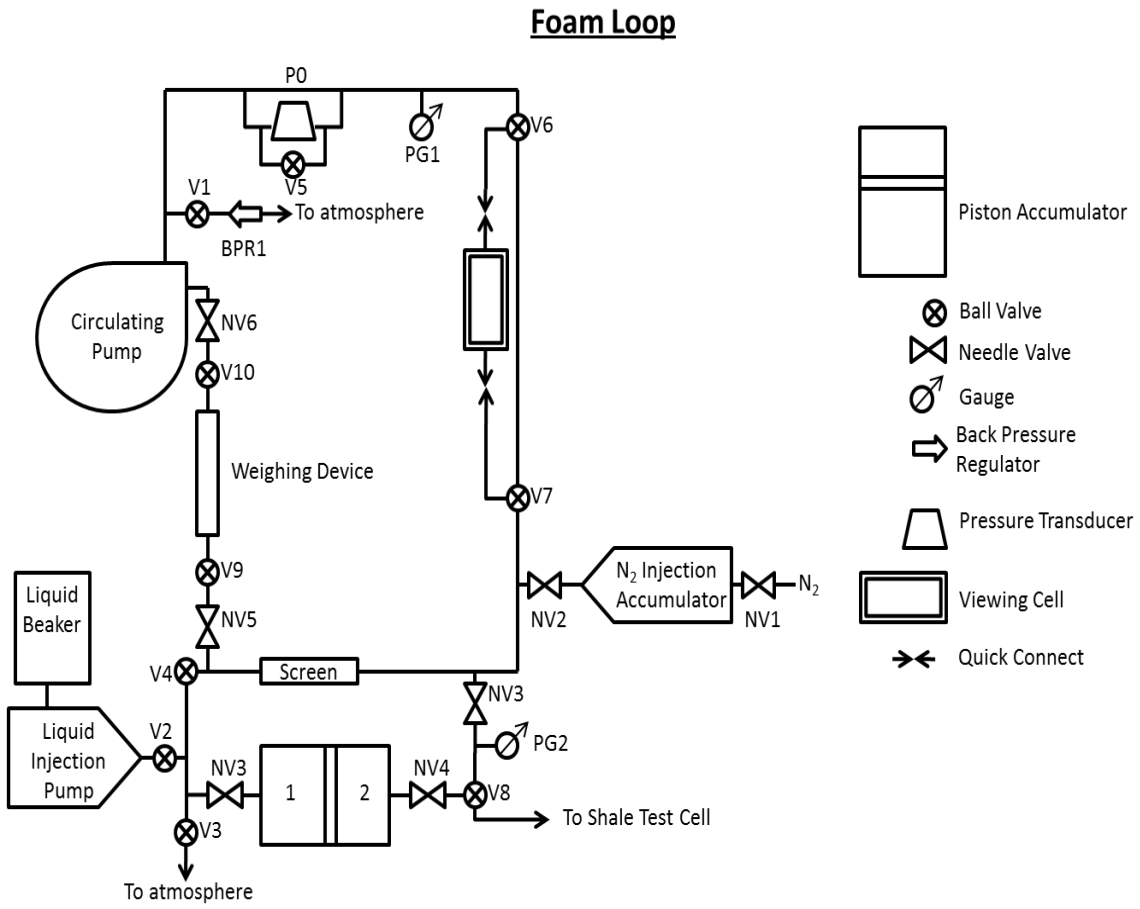

Figure 3.2 Flow Diagram of Foam Flow Loop

3.1.1 Pumps

Liquid Injection Pump

The liquid injection pump is a standard piston pump; this one had a maximum rate of 24mL/min and a maximum pressure of 10,000 psi, although this was never tested. It is a Beckman Model 100A. All liquids delivered to the system went through this pump. This pump injects the initial liquid solution into the flow loop

Circulation Pump

For foam circulation a Micropump gear pump was used. The gears were driven by a magnetically coupled 1 hp electric motor and capable of flow rates up to 2 gallons/min and pressures up to 2,000 psi. This pump circulates the liquid and foam inside the flow loop.

Manual Pump

To set the initial downstream pressure a manually operated piston screw pump has been used. It has a capacity of 48mL and a maximum pressure of 10,000 psi.

3.1.2 Back Pressure Regulators

BPR1

This back pressure regulator is a heavy duty backpressure regulator. Although pressures were very low in the system, the diaphragm material needed to be more robust. A TEFLON diaphragm back pressure regulator was initially installed but the foam flow through the regulator eroded the diaphragm inhibiting the device to seal. Thus a TEMCO Inc. BPR-50 with a 5,000 psi working pressure was installed with a stainless steel diaphragm. This back pressure regulator is used to hold a constant pressure inside the foam loop while foam is being generated; it allows gas and liquid to escape while adjusting the gas liquid ratio inside the loop.

BPR2

A Mitey Mite 91XW back pressure regulator with a TEFLON diaphragm was used, unlike BPR1, due to a lower velocity flow rate of the foam through the regulator. This regulator holds pressure constant inside the shale test cell while foam is flowing from the accumulator

3.1.3 Volume Apparatus

N2 Injection

To control the amount of gas injected, an accumulator is used. This accumulator is a 500mL accumulator with a maximum pressure of 3000 psi. It is without a piston inside and has needle valves on either side (NV1 and NV2).

Viewing Cell

The viewing cell used is a custom made piece of equipment. It is depicted in Appendix A in Figure A.3, and is constructed out of a pipette enclosed in hardened acrylic and has been pressure tested up to 1,000 psi. The viewing cell is a direct indication of the homogeneity of the foam as the quality is increased. It also allows for the measure of the stability of the foam by connecting quick-connect fittings to both sides and capturing foam at high pressure and measuring the time it takes for the foam to break down.

Weighing Device

The weighing device is also a custom made piece of equipment. It is a ¾" section of tubing with a needle valve outside a ball valve on both sides as shown in Appendix A in Figure A.4. It is used to measure the density of the foam and ensure a consistent foam quality between foam tests.

Liquid Beaker and Seawater Reservoir

These are simply 1000mL beakers containing liquids to be injected into the system.

Piston Accumulator

The piston accumulator is used to flow liquid and foam across the shale surface in the shale test cell. It is a 1000mL accumulator with a PTFE piston. The liquid injection pump pushes the piston to push either seawater or foam to the shale cell.

Shale Test Cell

To expose shale to fluids at pressure, a shale test cell has been created to seal a shale sample without crushing it. Shale is surrounded by a hardened epoxy and in then placed inside the shale test cell. Figure 3.3 following is a detailed drawing of the shale test cell.

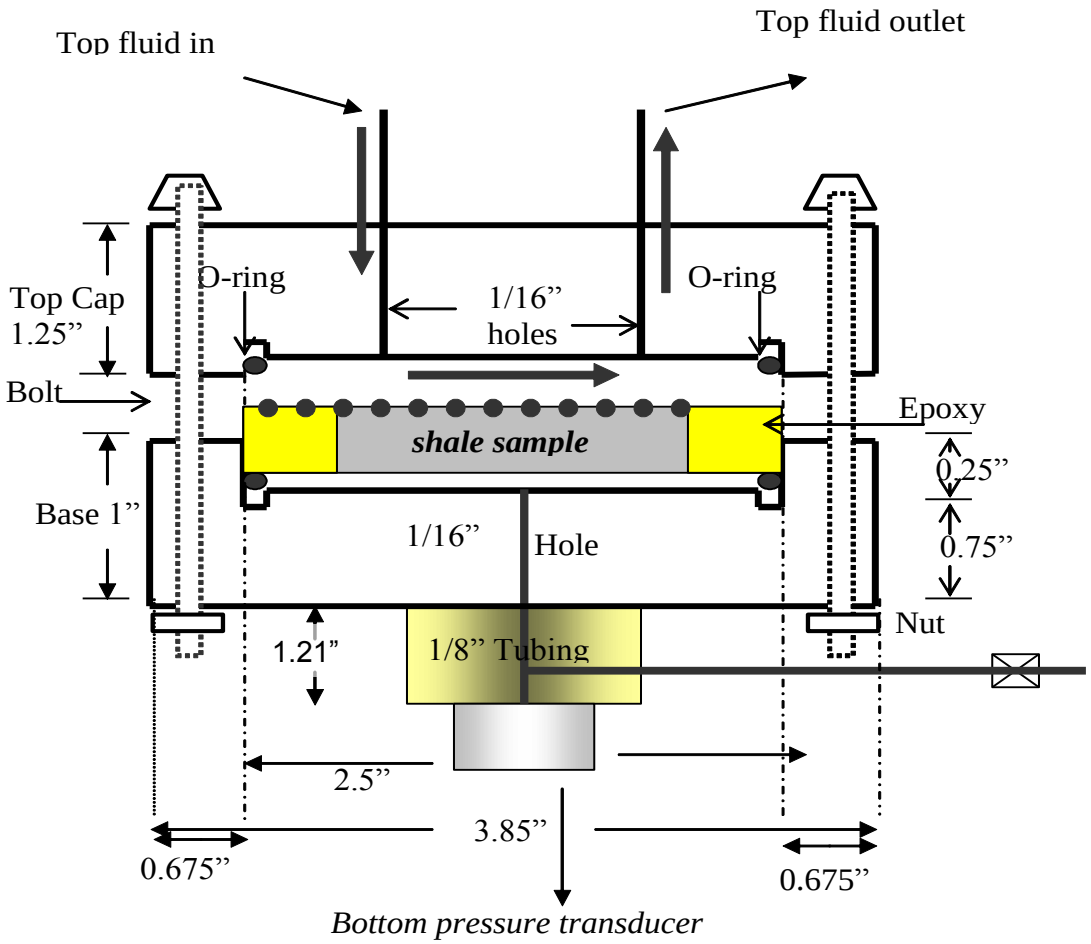

Figure 3.3 Shale Test Cell Diagram

Foam Generator/Screen

Mixing is achieved using a 140 micron screen inside a tubing filter. Originally a beadpack with 180 micron beads was installed, but pressure drop across the beadpack was too high for the pump to push fluids through.

3.1.4 Pressure Measuring Devices

PG1 and PG2

Pressure gauges used to monitor loop pressure (PG1) and foam injection pressure (PG2).

3.1.5 Pressure Transducers

P0

Valadyne style diaphragm pressure transducer used to measure the pressure differen across a set length of tubing. This pressure measurement used to calculate viscosity. Calibrated for a pressure range of 5 psi.

P1 and P2

Valadyne style pressure transducers measuring inlet and outlet pressures on the upstream side of the shale test cell. Calibrated for a pressure range of 500 psi.

P3

Strain gauge style pressure transducer used to measure the downstream pressure of the shale test cell. This is the most important measurement and so the strain gauge must be accurate and precise. The measurement is read in a very small closed volume to get the best accuracy as possible. Calibrated for a pressure range of 500 psi.

3.1.6 Valves

V1-V12

Ball valves are predominantly used, two-way allowing only for open and closed settings. Three way valves allow for changing flow pathways.

NV1-NV6

Needle Valves specifically placed to allow for precise control of flow through these valves.

3.2 PROCEDURE

In order to compare shale samples, a base seawater test is performed on every shale sample before the foam testing commences. For every shale sample, the seawater test is run first, followed by a foam test, and lastly followed by a NP foam test. After both foam tests are performed, the stability of the foam is measured. During the foam generation, when homogeneous foam has been produced, measurements of the pressure drop across the line are taken to calculate the viscosity. The following sections describe the procedure used during these tests.

3.2.1 Shale Sample Preparation

The following section describes the steps to produce shale samples to be used in the shale test cell.

1. Take the shale core and cut a section 12 inches in length. Then take the 12 inch section and cut a rectangular prism of dimensions: 1.3" x 1.3" x 12"

2. Clean the surface of the aforementioned shale section with hexane. Place this section of shale onto a 2.5" x 2.5" x 0.5" square base (the base material can be anything but wood or clear PVC work best). Make sure the section is placed so the 12" edge is normal to the base. When the section is level and upright, encase the shale with a 2" I.D. clear PVC tube that is 18" long and use epoxy to fix the pipe to the rectangular base. With the shale inside the PVC, fill the PVC pipe with epoxy to the top of the shale section form a supporting structure for the shale.
3. When the epoxy reaches the top of the shale section, place an object of low value on top of the shale that fits inside the remaining part of the epoxy. Fill the remaining space inside the PVC pipe with epoxy.
4. Wait a week for the epoxy to cure, then using an oil wet saw, cut the PVC into 0.25" slices to be used inside the shale test cell. After each cut, submerge the slice in an oil bath.
5. Remove the PVC casing around each sample and place them in a desiccator to reach equilibrium with the set water activity inside a desiccator.

3.2.2 Screen Wire Construction

In order for foam to flow over the shale sample in the shale test cell, screen wire discs must be used. If more viscous fluids will be used, screen wire with larger hole-size should be used.

1. With a piece of both 240 mesh and 400 mesh screen wire, outline a shale sample using a permanent marker. You will need two of these so follow this procedure twice.

2. Spread a very thin layer of epoxy over the outline made from the permanent marker. This layer should be approximately 0.5 cm wide.
3. When the epoxy is dry, cut out the screen wire disc and shave the edges so that the screen wire disc will not touch an o-ring when placed inside.

3.2.3 Sealing Shale Sample in Shale Test Cell

In order to generate quality data, a secure seal is needed between the shale test cell and the shale sample. Without it, all data generated is useless. It is imperative to follow the following procedure exactly.

1. Place the bolts with locking washers in the bottom half of the shale test cell, slowly and carefully turn over the shale test cell so that the bolts are held upright by the table underneath.
2. Place the o-ring and screen wire disc (with the number 400 side facing up) in the bottom of the clean bottom half of the shale test cell with the bolts sticking up and through the bottom half. Make sure the screen wire is small enough and not touching the screen wire (this can cause a leak).
3. Carefully place the shale sample on top of the o-ring and screen wire disc without moving the screen wire disc. Then place the second screen wire disc (with the number 400 side on the bottom) on top of the shale sample so that the screen wire will not touch the o-ring in the top half.
4. With the o-ring in the top half of the shale test cell, place the top half of the shale test cell on the shale sample making sure all of the bolts slide through their proper holes in the top half.

5. With the top half of the shale test cell on, place the washers and nuts on each bolt and finger tighten the nuts on each bolt. Using a star pattern begin to tighten the bolts using a crescent wrench and a driver. Tighten the bolts until firm, make sure the bolts are not tightened in large steps. Go around 2-3 times before the bolts are firmly tightened.
6. Use a crescent wrench and a torque wrench, using the star pattern again, torque the bolts to 75 lb-inches. Ensure a constant gap is formed between the top and bottom half of the shale test cell all the way around to so that a seal has been produced. The top and bottom halves should lay flat on the shale sample.

3.2.4 Seawater Base Pressure Penetration Test

1. Prepare a 1,000mL solution of seawater in a beaker. Mix 960g of water with 40g of sea salt to obtain a 4% by wt. seawater solution.
2. Completely fill up side 2 of the accumulator with the seawater solution.
3. Place shale sample in shale test cell with o-rings and screen wire discs on either side of the shale sample. Tighten down the bolts to 75 lb-in of torque and make sure the discs shale test cell plates are flat against each other to ensure and o-ring seal with the shale sample.
4. Place the shale test cell in an oven to prevent temperature fluctuations and hook up the flow lines to the shale test cell.
5. Make sure the liquid beaker has at least 1000mL of de-ionized water in it and valves NV3, NV4, and V2 are open. V8 must be directed towards the shale test cell. V12 and V3 must be closed.

6. Set pump to maximum flow rate and pump seawater through the shale test cell. Make sure there is only water coming out of the outlet of BPR2 and at a steady rate, usually takes 2-5 minutes.
7. Set BPR2 to 300psi and again flow until there is a steady stream of water coming out of the outlet of BPR2. Using the manual pump set P3 (downstream pressure) to 50 psi. Slowly decrease the flow rate of the pump until a drop every 5 seconds is coming out of the outlet. Start recording the data at the computer.
8. When P3 (downstream pressure) becomes equal to the P1 and P2, stop the test and analyze the data to calculate permeability of that test.

3.2.5 Foam and Foam with NP's Pressure Penetration Tests.

These tests are identical except for the starting liquid injected.

1. Make up the liquid solution to be injected into the flow loop. For regular foam mix 0.3g of SDS per 100mL of de-ionized water. Dilute NP solution to desired NP concentration with de-ionized water. Then add 0.3g SDS per 100mL of solution. Fill side 1 of the piston accumulator completely with seawater (volume of side 2 is 0).
2. Raise the N2 accumulator pressure to 500psi opening NV1, while keeping NV2 closed. Open V4, V2, V1, V5, V9, V10, NV5, and NV6. Make sure V6 and V7 are set to flow through the viewing cell. Close NV3, NV4, and NV7 and make sure V8 is directed toward the flow loop.
3. Make sure a clean beaker is at the outlet of BPR1 to catch the extra solution during initial injection. Set the pump to maximum flow rate and start pumping in the liquid solution for foam generation. Pump and redeliver liquid solution for 30 min or until all air is out of the flow loop.

4. Set BPR1 to 350psi and let the pump continue to run until PG1 reads 350 psi. Once PG1 reads 350psi stop the pump and start up the circulation pump. The circulation pump should be kept below 1000 rpm's to for safety (700-900 rpm).
5. Circulate the pump until P0 is at a constant level. Then open V5 and slowly inject N2 by opening NV1 while keeping NV2 closed. Once NV1 is all the way open, shut it completely and open NV2 to set the accumulator pressure back to 500 psi. Close V5 and once again turn on the circulation pump to the same rpm setting as before.
6. Repeat Step 5 until the foam circulating through the viewing cell is homogeneous. When the circulation pump is stopped, there should be no liquid layer in the bottom of the tube. Adding more N2 to the foam loop past this point can vapor-lock the pump.
7. To calculate density or quality of the foam, while the circulation pump is off, close NV5, NV6, V9, and V10. Then disconnect the tubing between NV6 and V10, and NV5 and V9. Then weigh the tubing with the foam inside and calculate density as described in section 3.3.2. The density should be around 0.3, which equates to a quality of 70%.
8. If the foam is homogenous and the quality is ~70%, record the rpm's and the P0 reading to calculate the viscosity.
9. Begin to fill up the accumulator by opening NV7 and make sure V8 is set toward the path of the accumulator. Slowly open V3 to allow a dripping of water to exit side 1 of the piston accumulator. With the circulation pump on, begin to inject more solution into the system at a very low rate. Keep the pressure reading of P0 constant while additionally solution is being injected. When the pressure drops to

325 psi. Shut V3, stop liquid injection, and turn stop the circulation pump. Inject N2 into the system to reach 350psi again.

10. Let the circulation pump run until P0 is constant again. Repeat Step 7 to check the quality of foam. Then repeat Step 9 until the amount of liquid that has exited from the piston accumulator is 750mL. As the pressure continues to drop as foam is filling up the accumulator, stop liquid and gas injection at a point where the final pressure in the system is 300 psi (this takes some practice and system know-how).
11. Close NV4 and NV7, and turn V8 so that it directs flow towards the shale test cell. Set BPR2 to 300 psi and slowly open NV4.
12. Use the manual pump to set P3 to 50 psi and close V11 once 50 psi is reached. Then turn on the injection pump with V2 and NV3 open and V3 and V4 closed. Set the pump to a low flow rate so that foam will drip out of the outlet of BPR2 at 1 drop per 5 seconds.
13. Record the data on the computer to calculate permeability.

3.2.6 Foam Stability Test

1. 1.After the piston accumulator is full, close V2 and NV3. Open V3 and fill a graduated cylinder, without letting the foam hit the sides, with 100 mL of foam.
2. Start a stopwatch as soon as the foam hits the 100 mL mark and record the time that the foam takes to completely break down.

3.3 Data Evaluation and Calculations

After generating data key parameters and calculations need to be performed to make this data usable. The permeability will be calculated in respect to the fluid imposed

on the shale. The viscosity will be calculated from the pressure drop across a pipe and the half-life calculated from interpolating a slope.

3.3.1 Permeability Calculation

Based on the work of Al-Bazali et. al. (2005) the following equation is used to calculate the dynamic permeability of each test.

$$k = \frac{m\mu CV}{A}(cm^2) \tag{3.1}$$

k: Permeability (cm^2)

m: Slope/3600 of the RED linear portion of curve (shown in Figure 3.4)

μ: Viscosity (psi.second)

C: Compressibility, psi^{-1}

V: Volume (cm^3)

A: Area, cm^2 (Surface area of the shale sample exposed to the upstream flow)

An example of the curve that generates the slope is as follows:

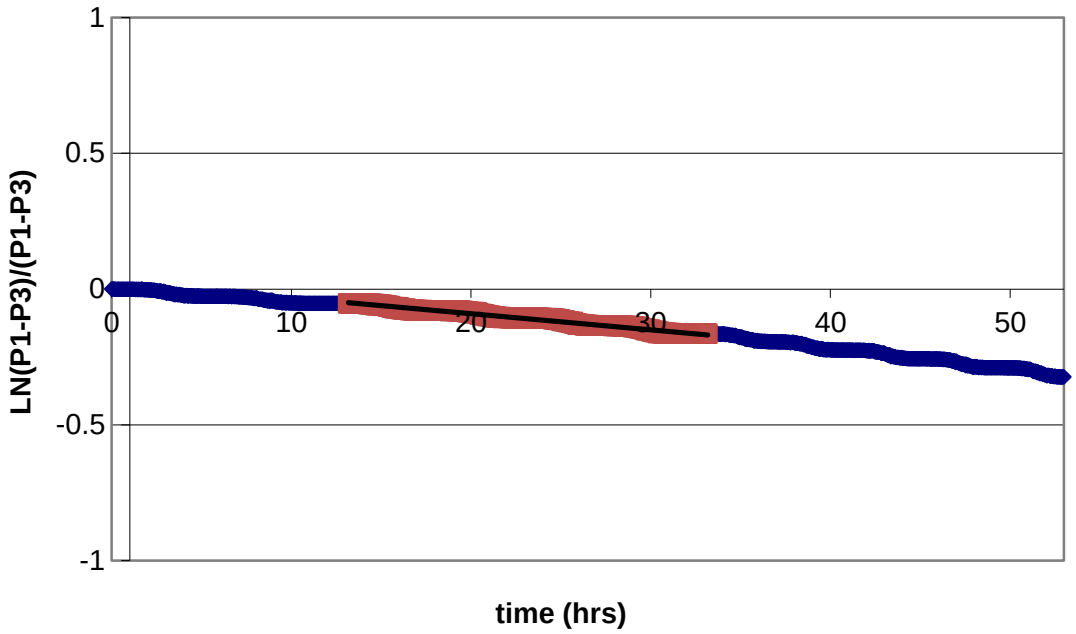

Figure 3.4 Transient Plot with Regression to Calculate Slope

The y-axis is equal to:

$$\frac{\ln(P1-P3)}{(P1-P3)} = \frac{\ln(upstream-downstream)}{(upstream-downstream)} \tag{3.2}$$

The x-axis is time in hours.

CHAPTER 4: RESULTS

4.1 ATOKA RESULTS

The first sets of tests to be presented are the Atoka Shale results from the Pressure Penetration Tests performed. Each test, as described in Chapter 3, has three subsequent steps. The first uses either tap water or seawater as the fluid injected and the permeability is calculated. The second step uses foam as the injection fluid and the third step is foam with the addition of NP's. From each fluid, permeability is calculated and is then compared with the other tests. Each test is labeled in this thesis using the final concentration of NP's added to the foam.

4.1.1 5% NP Foam

The first step in this test used tapwater as the injection. The results are plotted below:

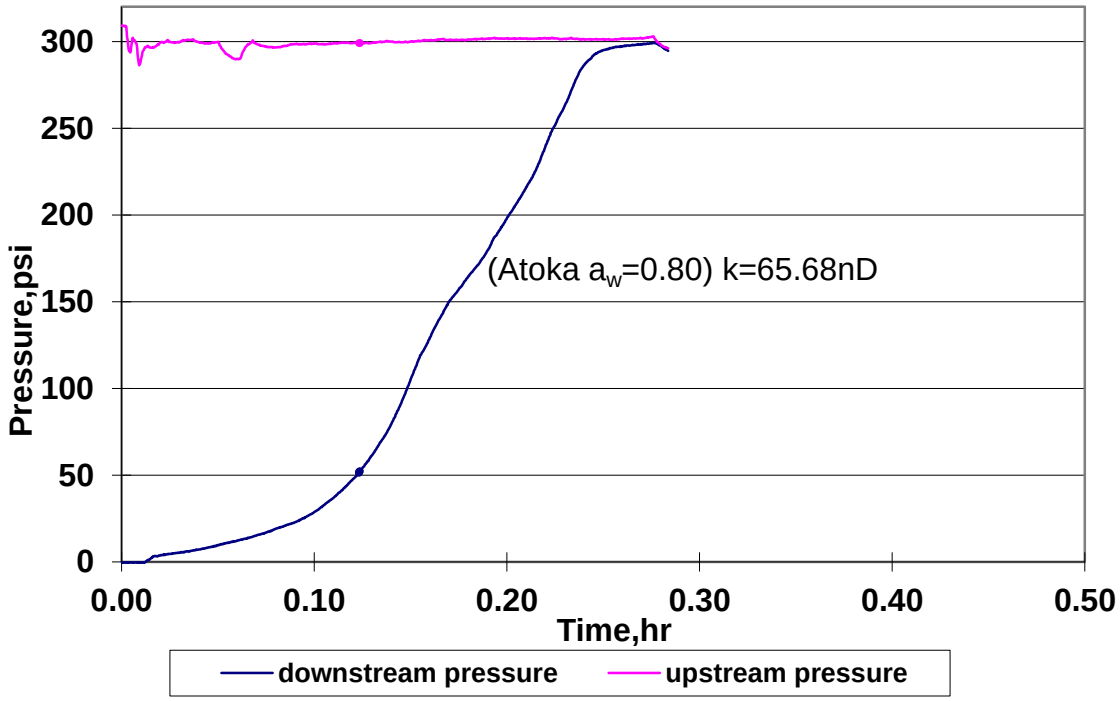

Figure 4.1 Atoka Shale with Tapwater

Figure 4.1 above shows a high permeability at 65.68 nD, this is most likely due to a small micro-fracture. The fluctuations in the downstream pressure further suggest the presence of a micro-fracture. Although evidence shows that a micro-fracture exists, without the use of a microscope, this cannot be verified. Therefore, the subsequent foam step was performed.

70 % quality foam was used as the injection fluid with the same shale sample used in Figure 4.1 above. Figure 4.2 shown below shows the results from the foam step of the Pressure Penetration Test.

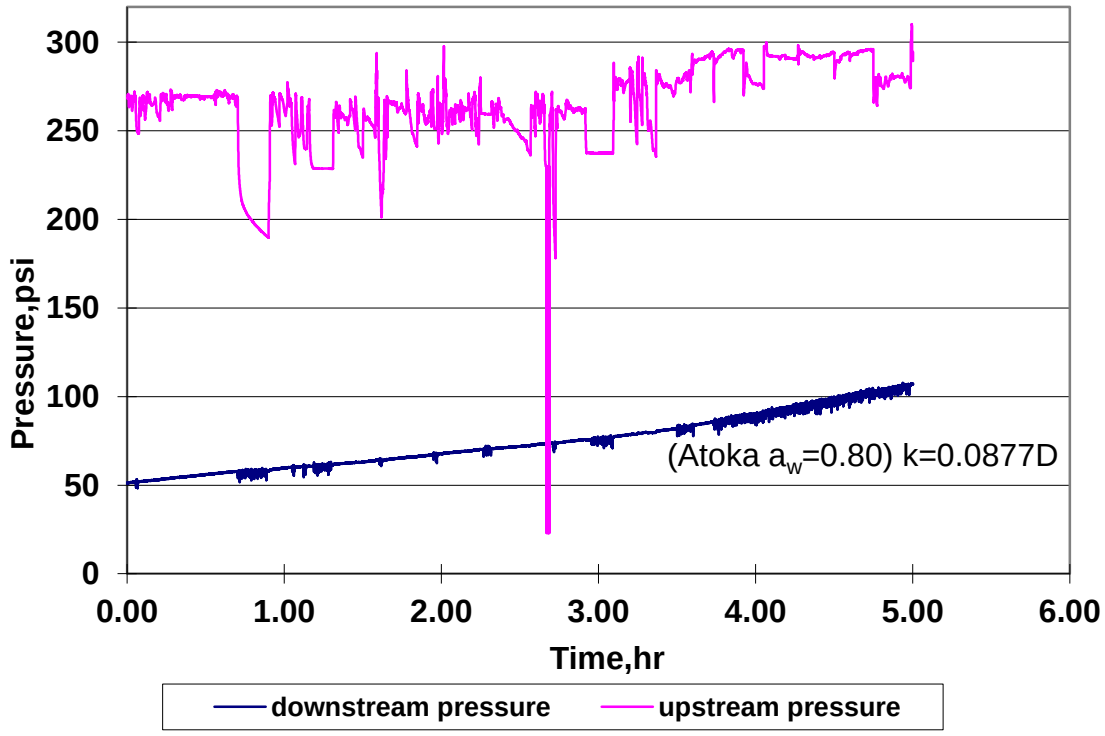

Figure 4.2 Atoka with Foam

Figure 4.2 shows the downstream pressure rise using foam as the injection fluid. The test only lasted 5 hours because the foam was fully consumed. The permeability calculated from this step was 0.0877 nD, much lower than the tap water.

Following the normal foam test, a test using foam with 5% NP's by weight as the injection fluid was performed. To be able to compare both foam steps, the foam quality was set at 70% again. Figure 4.3 shown below displays the results from this step.

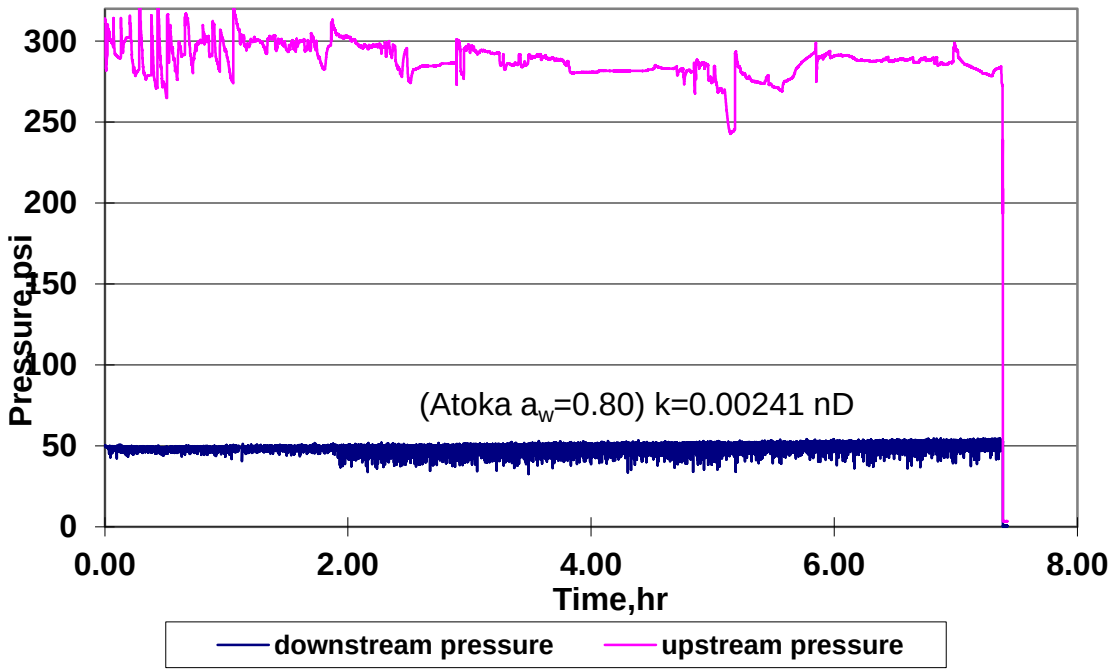

Figure 4.3 Atoka with 5% NP Foam

Figure 4.3 above shows that pressure barely increased at all, resulting in a very low permeability of 0.00214 nD. Figure 4.4 below show each step in the test on the same graph for comparative purposes.

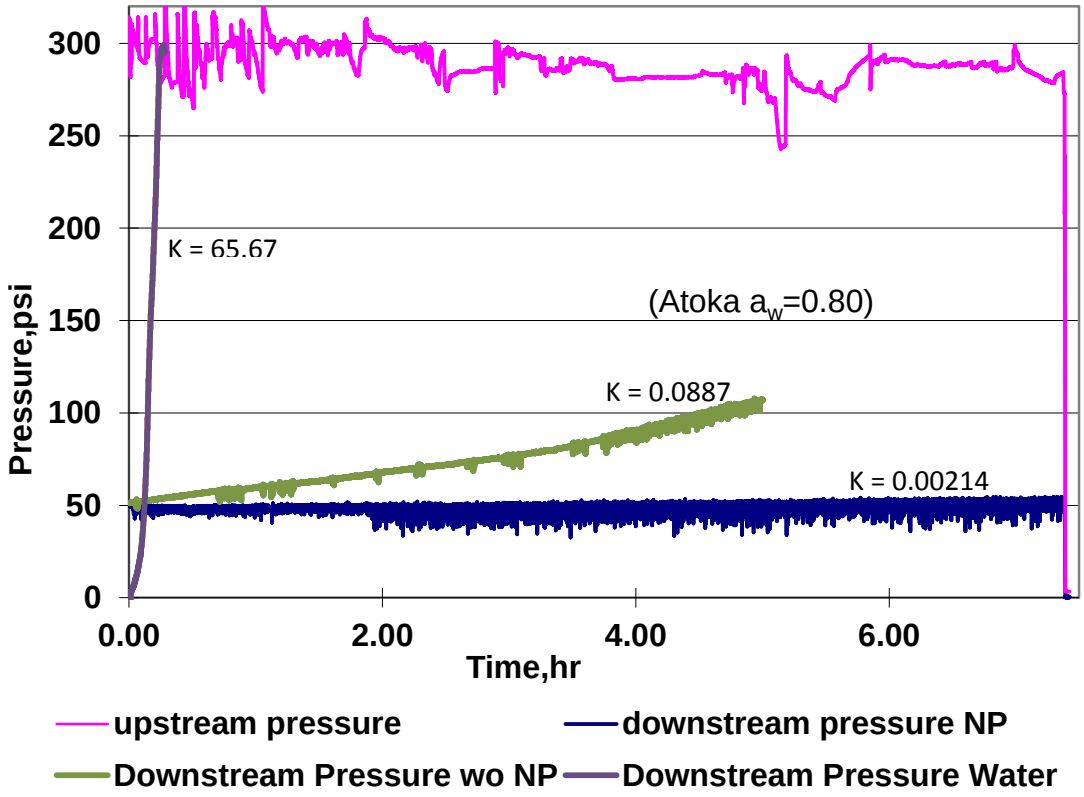

Figure 4.4 Three Step 5% NP Foam Test

Figure 4.4 above shows the reduction in permeability between each of the steps. The extremely large reduction from the tap water step to the foam step is most likely due to a micro-fracture in the shale sample. The smoothness of the foam curve indicates that the foam does not flow through the micro-fracture and the true permeability of the shale is measured. Furthermore, the foam with 5% NP almost completely plugs off the shale with an extremely low permeability of 0.00214 nD.

4.1.2 2% NP Foam

Again the first step of the test used tap water as the injection fluid. Figure 4.5 below shows the results from this step.

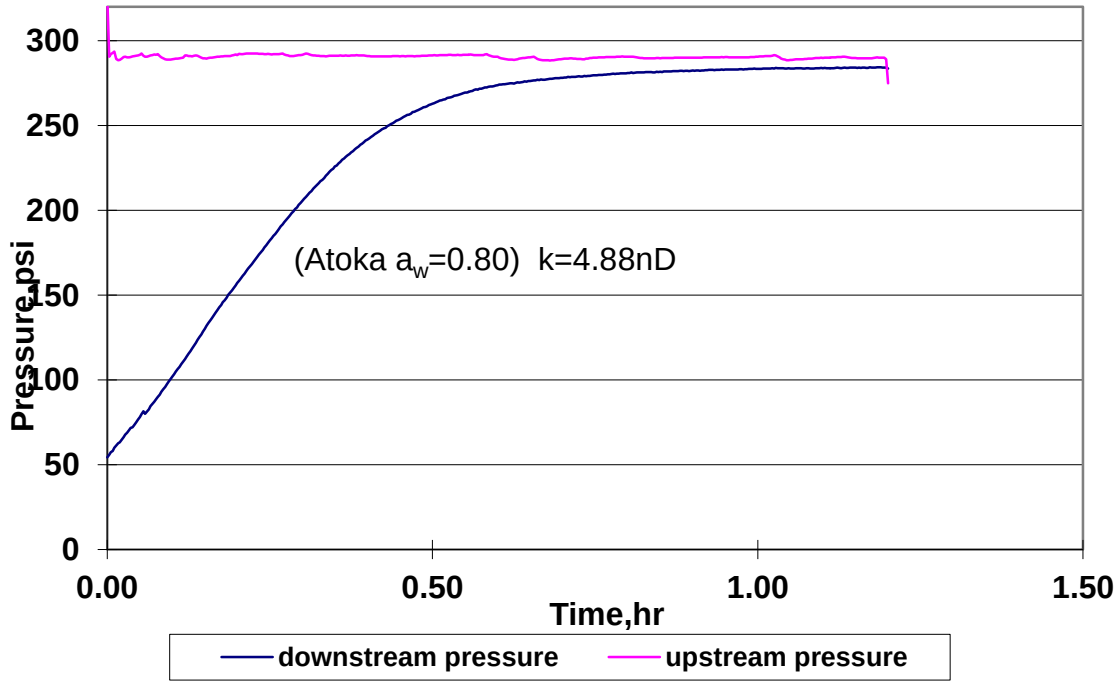

Figure 4.5 Atoka with Tapwater

Unlike the first step of the previous test with tap water, the permeability is much lower, indicating that this sample of shale is not cracked. From past experience, Atoka shale with water as the injection fluid has a permeability range approximately between 1 and 10 nD. Moving on to the next step of the test using foam, Figure 4.6 is shown below.

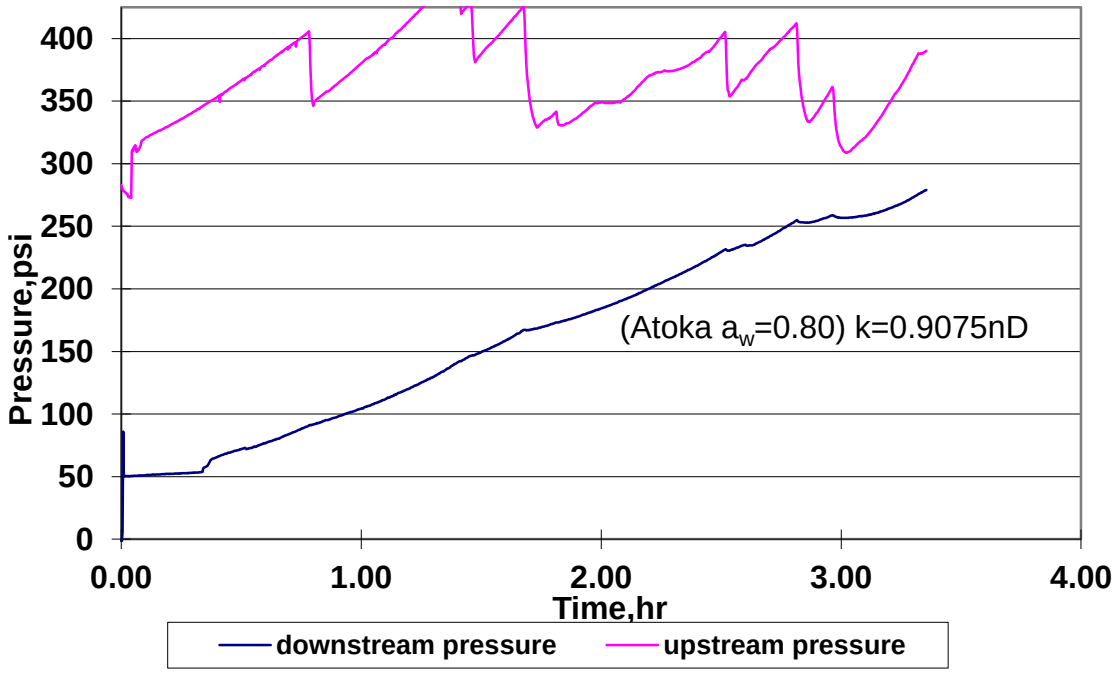

Figure 4.6 Atoka with Foam

The variation of the upstream pressure above is due to injecting the foam to the shale test cell using a needle valve and opening it manually. The needle valve was extremely sensitive and a turn of only a few degrees could raise pressure 20-50 psi. The curve above is not a smooth curve with a few spots of rapid increase. The likely cause of this roughness could be due to a small micro-fracture developing. With the successful results shown above, the third step of the test was performed using foam with 2% NP as the injection fluid. Figure 4.7 shown below displays the results from this step.

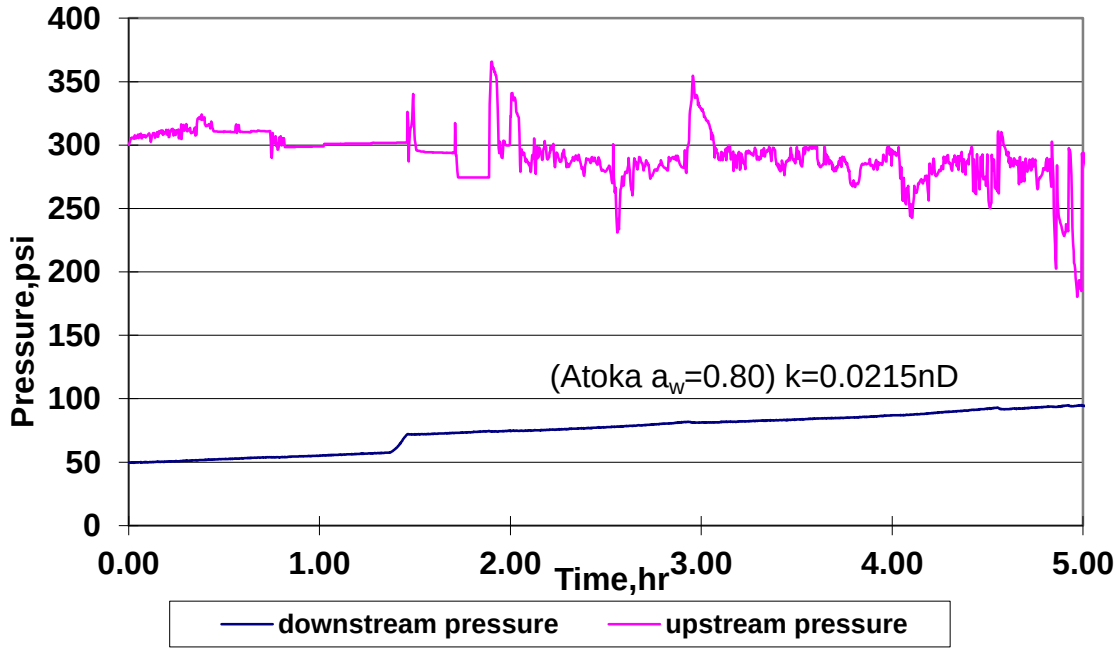

Figure 4.7 Atoka with 2% NP Foam

Figure 4.7 above has a point in the downstream pressure where a rapid increase occurs. The cause of this could be the opening of a small micro-fracture in the shale, of which then closed up. This jump confirms the speculation from the previous foam step. The most interesting graph in this series is the graph comparing all three curves together. The NP's are behaving as predicted and large reductions in permeability can be observed.

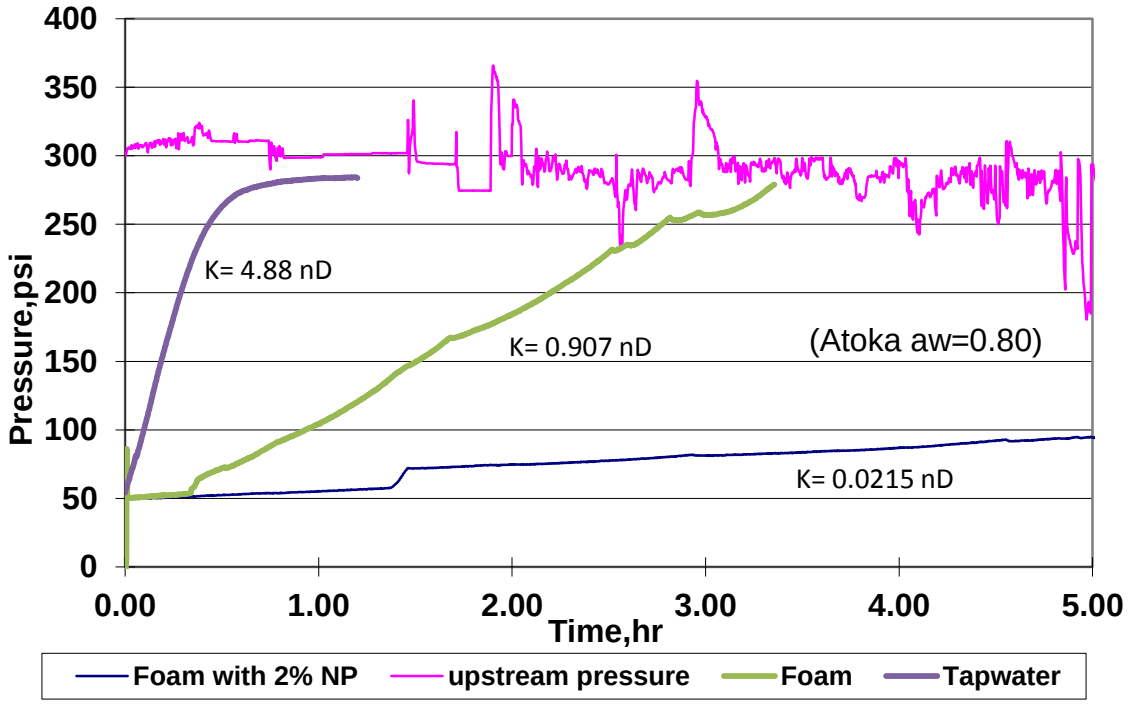

Figure 4.8 Three Step 2% NP Test

From Figure 4.8 above, each successive step in the test displayed a lower permeability, about a whole order of magnitude. After this three step test, a 1000 mL accumulator was installed to allow more control on the flow rate of the injection fluids as well as allowing more foam to be produced for longer tests.

4.1.3 1% NP Foam Results

The three step test using 1% NP foam as the last step was the first full set of steps to include a 1000 mL accumulator in the flow loop. The following steps were much longer compared to the previous tests. Also, there was a large period of time when all of the samples of shale tested were found to be cracked or fractured. Figure 4.9 below

shows the first step in our test using 4% by weight seawater (4% refers to the amount of sea salt added to water).

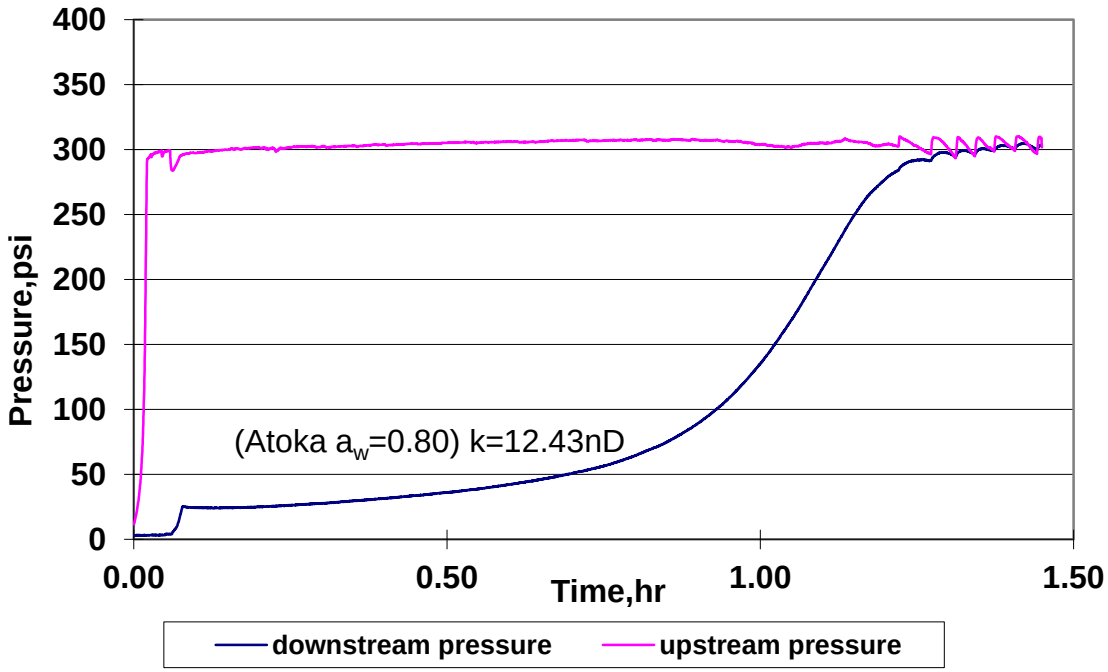

Figure 4.9 Atoka with Seawater

Figure 4.9 above shows another Atoka shale sample with seawater as the injection fluid. To combat extra effects due to osmosis, seawater is now used. Seawater has a water activity of 0.98, closer to the water activity of the shale than the tap water previously used. The permeability is a little high, so it is possible the calculated permeability is influenced by a small micro-fracture. It is very close to the generally accepted permeability range resulting in continuation to the foam step of the test. The results from this foam test are shown below in Figure 4.10.

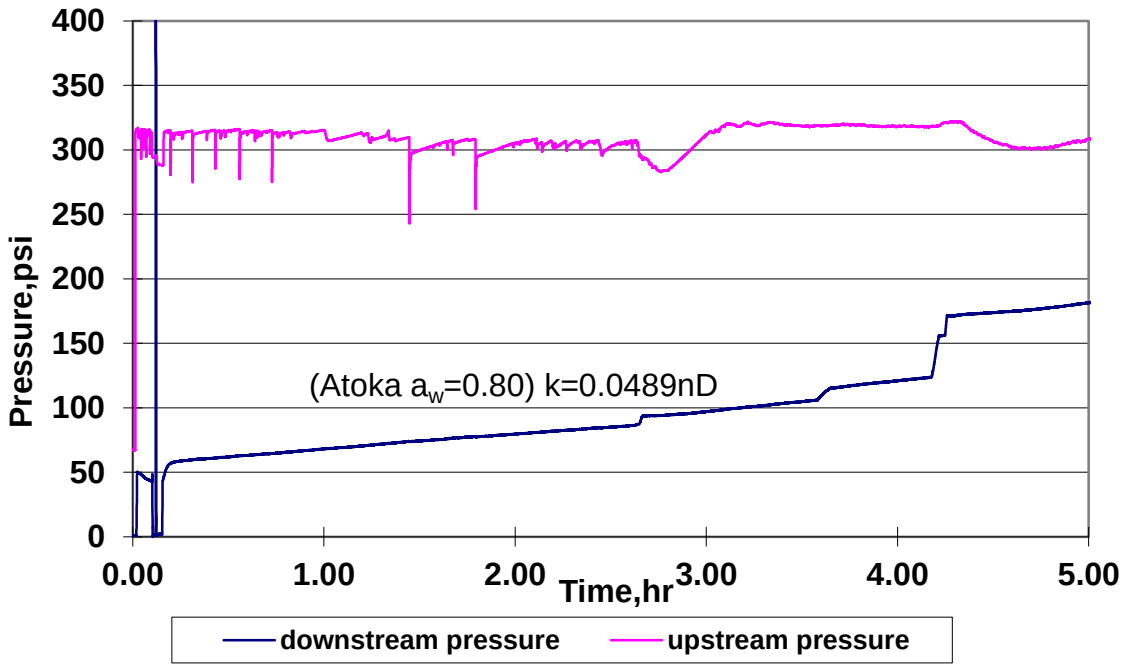

Figure 4.10 Atoka with Foam

As with the other samples, the points of rapid pressure increase are most likely due to small micro-fractures in the shale sample. The smooth parts of the slope however are representative of the fluid flowing through the shale pores. The relatively high entrance pressure of nitrogen restricts the foam from using small micro-fracture as a continuous conduit for flow. The third step of this test using 1% NP foam is shown below in Figure 4.11.

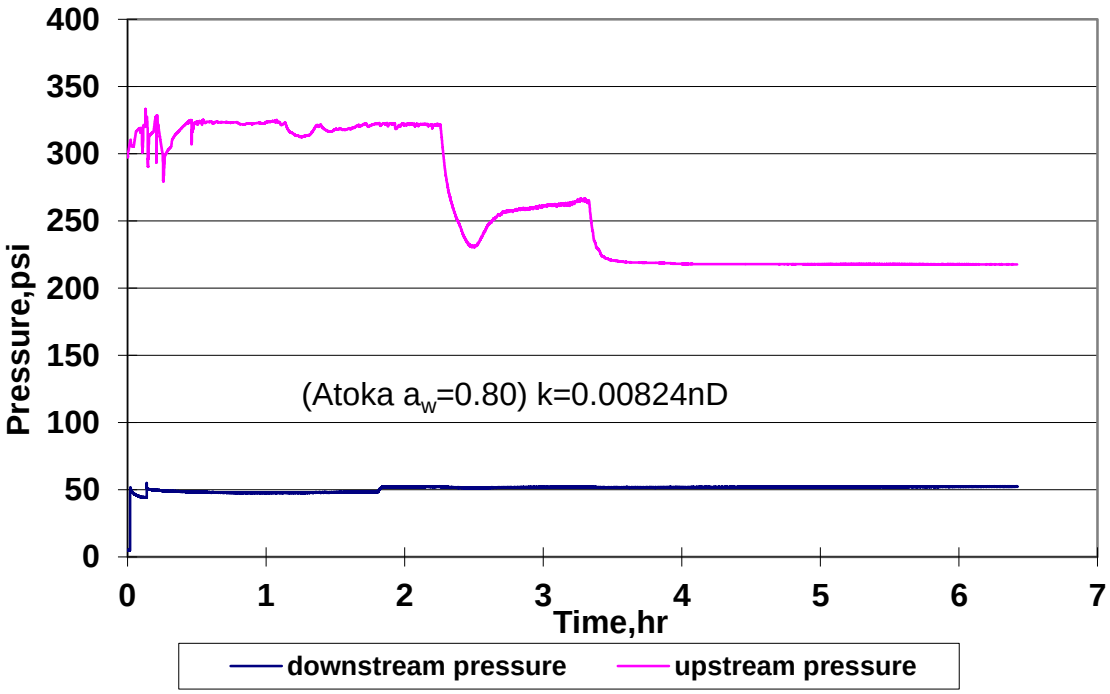

Figure 4.11 Atoka with 1% NP Foam

Figure 4.11 shows that the foam all but plugged up the shale sample, the permeability reduction from normal foam is still almost a whole order of magnitude smaller even at 1% NP concentration in the foam. The drop in pressure in the upstream from is most likely due to a small leak in the back pressure regulator. This can occur when NP's build up around the seal inside. If the back pressure regulator becomes stuck open, the compressibility of foam will cause the foam to flow at a high rate out of the accumulator, hence the relatively short duration of this step. To properly compare the three steps of the test, Figure 4.12 is shown below.

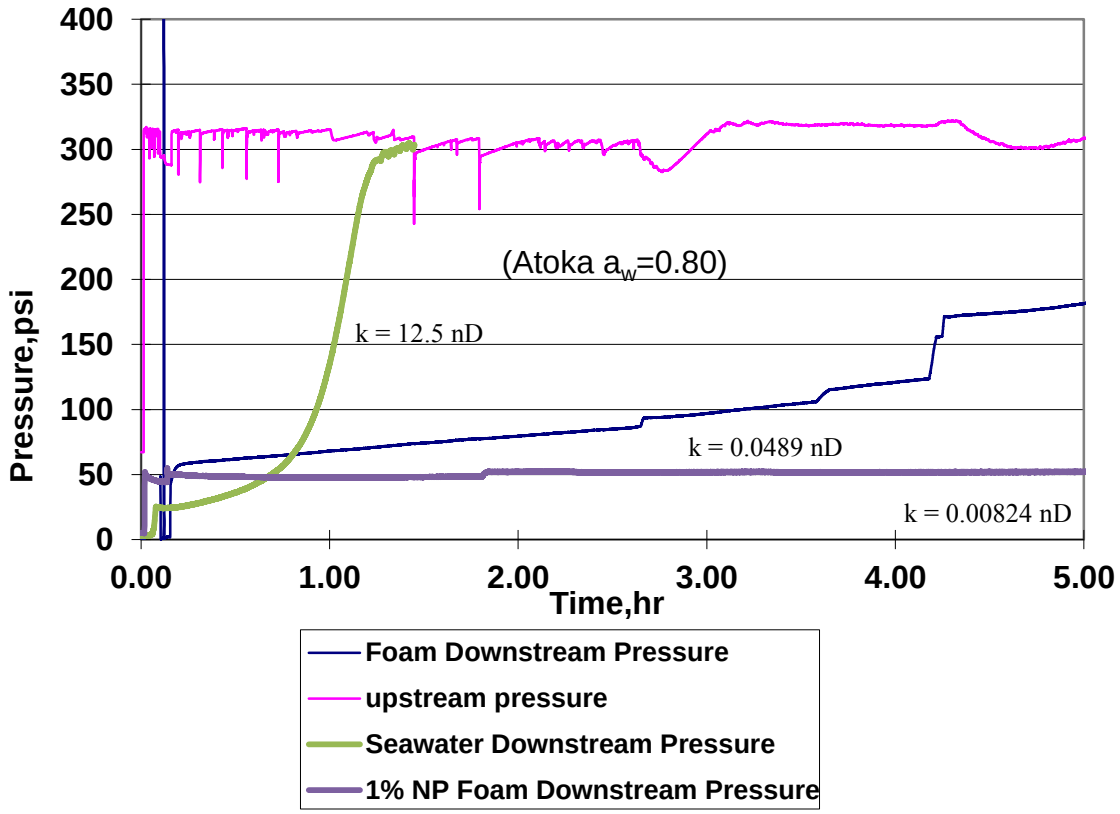

Figure 4.12 1% NP Foam Three Step Test

Like the earlier tests the permeability of each subsequent step in the test displayed a significantly lower permeability. The 1% NP foam reduced the pressure transmission through the shale sample to an increase of 2 psi in 5 hours.

4.2 TGS Results

Initial plans for the TGS were to run a set of tests matching the set of tests on the Atoka shale. When running the TGS samples, large micro-fractures were found to be in most of the samples. Appendix A will introduce some plausible causes for these

fractures to occur in the shale. However, one sample was found that was believed to be unfractured. The results for this test are as follows.

4.2.1 2% NP Foam

Without any other TGS results to compare to, the following test is thought to be a true permeability reading of the rock and not a microfracture. Following these results, pictures of the sample will be included supporting the unfractured assumption. The first step of the 2% NP foam test using the TGS is seawater for comparison to all the other shale samples used. The results are shown in Figure 4.13 below.

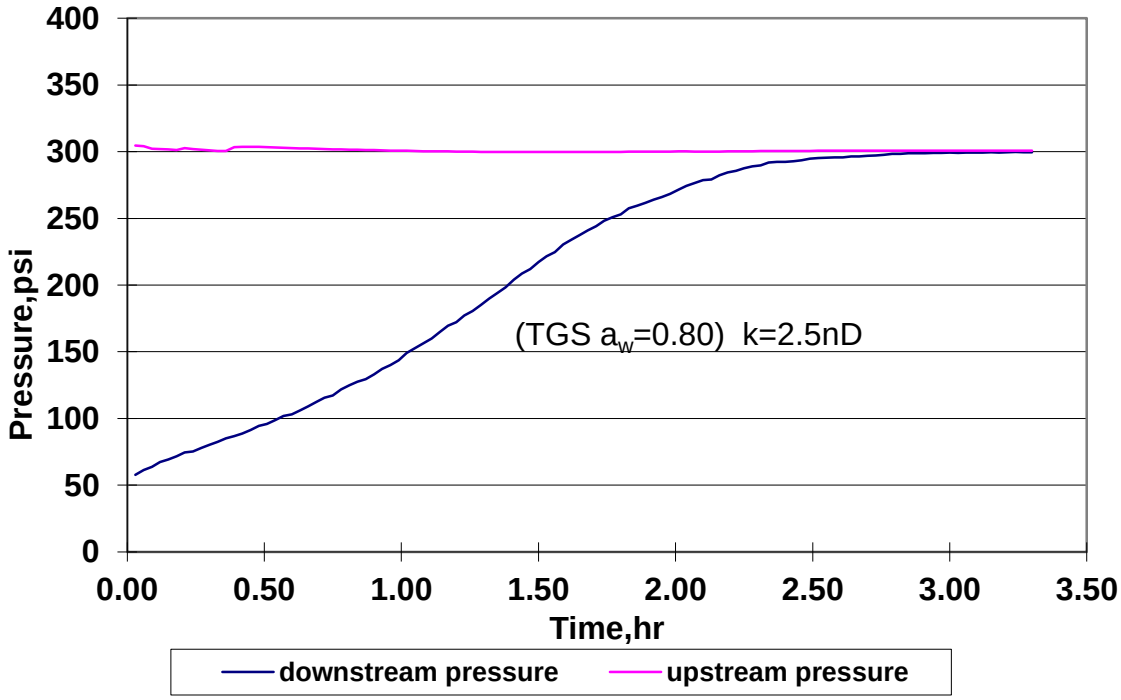

Figure 4.13 TGS with Seawater

The permeability calculated from this test is in the normal permeability range for shale as we have seen in the past. Although this kind of test has never run before using

reservoir rock, the pore sizes should be similar in size with Atoka shale and therefore the permeability should be similar to what has been seen with Atoka Shale. The next step in the test is using foam as the injection fluid. Figure 4.14 shown below are the results of using 70% quality foam.

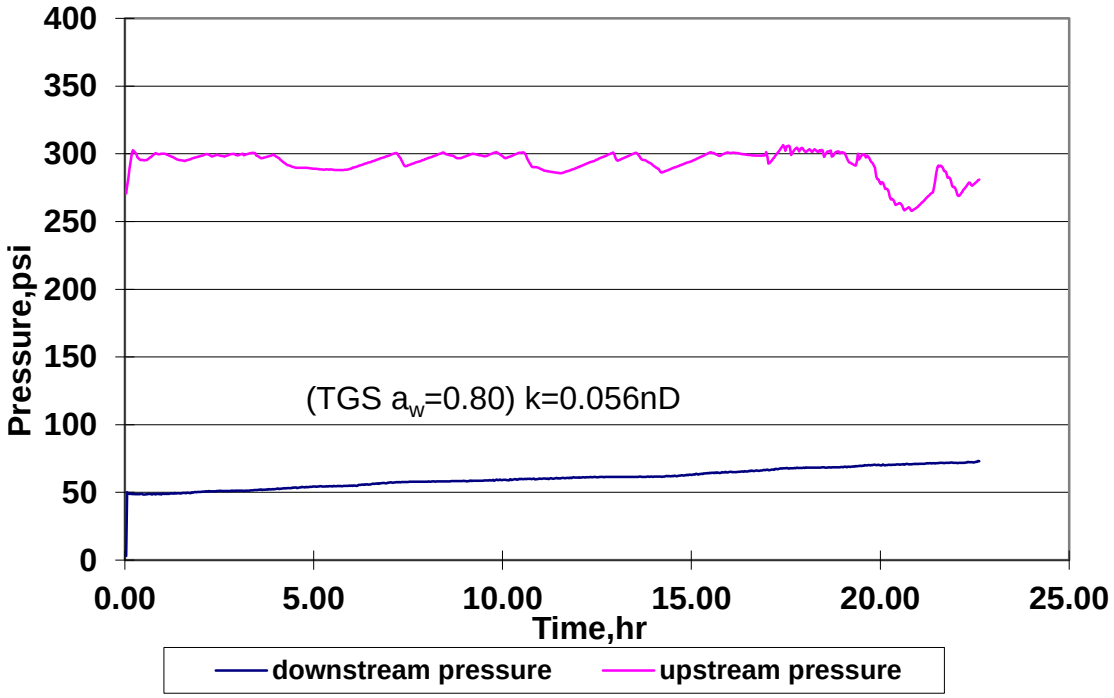

Figure 4.14 TGS with Foam

The above figure shows the test ran for about 23 hours. This is much longer than the previous tests due to the use of a more accurate and precise injection pump. At 23 hours the 1000 mL accumulator was empty. With the TGS sample, foam displayed a very low permeability, so low the upstream and downstream pressures did not equilibrate. The next step in the test is to run the 2% NP foam as the injection fluid. A very small

permeability was expected for the NP foam due to the already small permeability shown with normal foam. Figure 4.16 shown below confirms these expectations.

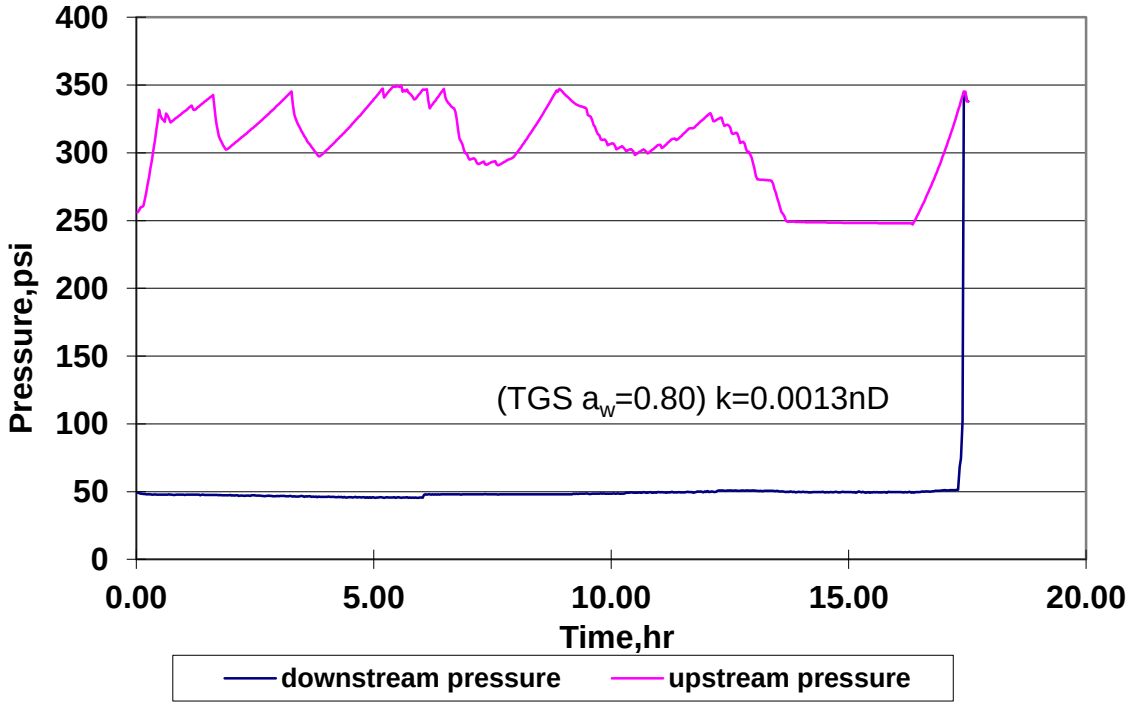

Figure 4.15 TGS with 2% NP Foam

2% NP foam was chosen for this test due to its successful results with Atoka shale. At this time, this was the only sample that was found to be unfractured. At first, the downstream pressure decreased from the initial set 50 psi. This can be a result of osmosis pressure differences between the seawater on the bottom of the Shale Test Cell and inside the shale sample. The test ended at 17 hours due to the shale cracking at the end. The upstream pressure increased rapidly due to the foam compressing, the shale fatigue point had probably been crossed and the shale cracked. There was, however, plenty of time to calculate a permeability from this step, k = 00013 nD. In order to

compare the previous TGS results, Figure 4.17 displays all three steps on the same graph shown below.

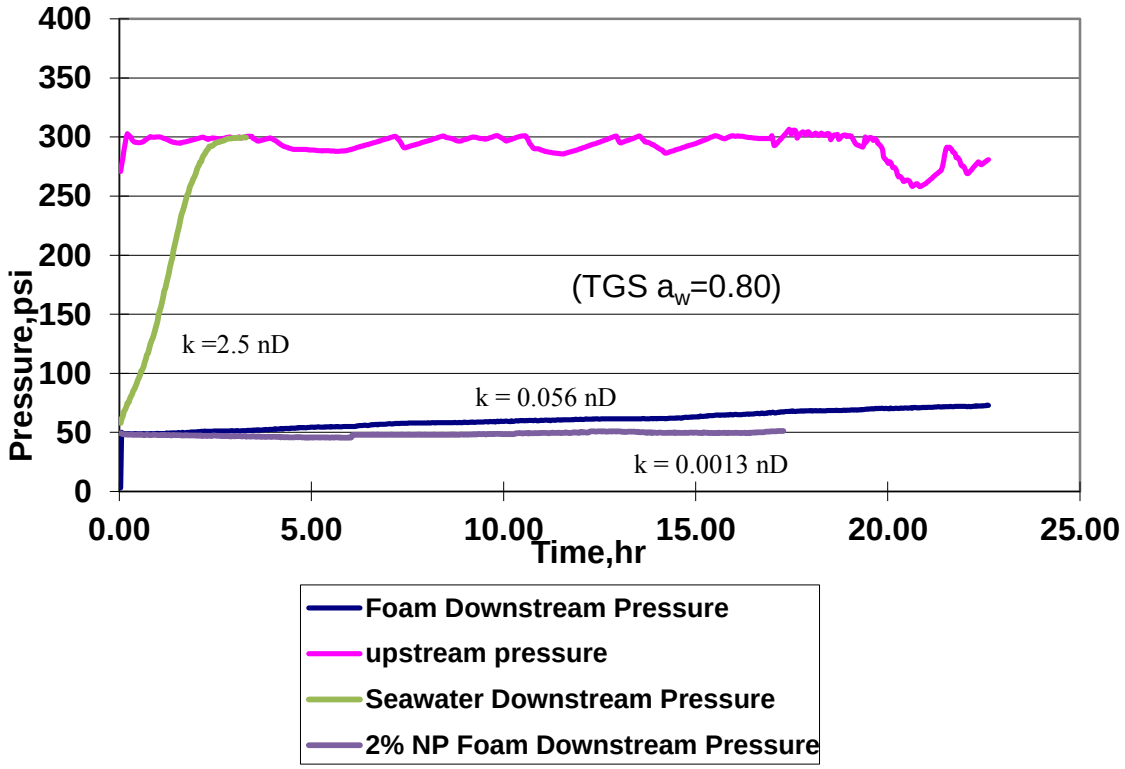

Figure 4.16 Three Step Test with 2% NP Foam

4.2.2 TGS with Drilling Mud

With this new type of shale, the assumption that the pores were being plugged by the NP's instead of just stabilizing the foam, another 3 step test was run using seawater, a water-based mud, and then the same water-based mud with 10 pounds per barrel (ppb) of NP's (the same NP's used in the foam in these tests). 10 ppb of NP's equates to approximately 1.7% by weight of NP's in the mud. The results from these tests are shown below.

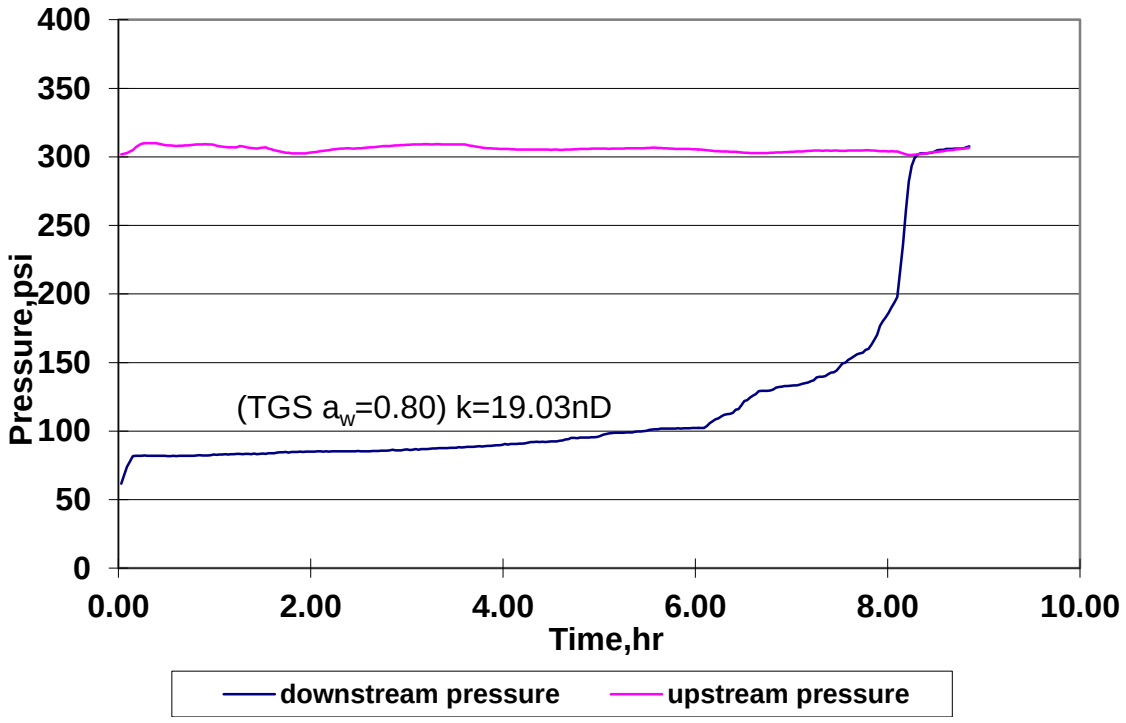

Figure 4.17 TGS with Seawater

Figure 4.18, above, shows the increase in pressure at the beginning of the test is normal. At about 6 hours the downstream pressure rapidly increased without flattening out. This is a great indication of a crack in the shale. The 19.03 nD permeability is an estimate from the steepest part of the curve. After the initial seawater step was run, a Darcy type flow experiment was performed. Pressure was held constant on the top of the shale and a flow rate was recorded using a graduated cylinder and a stopwatch. After which, the permeability of the "crack" was calculated. Figure 4.19 are the results from the Darcy test that held 200 psi constant as the upstream pressure and atmospheric on the downstream pressure.

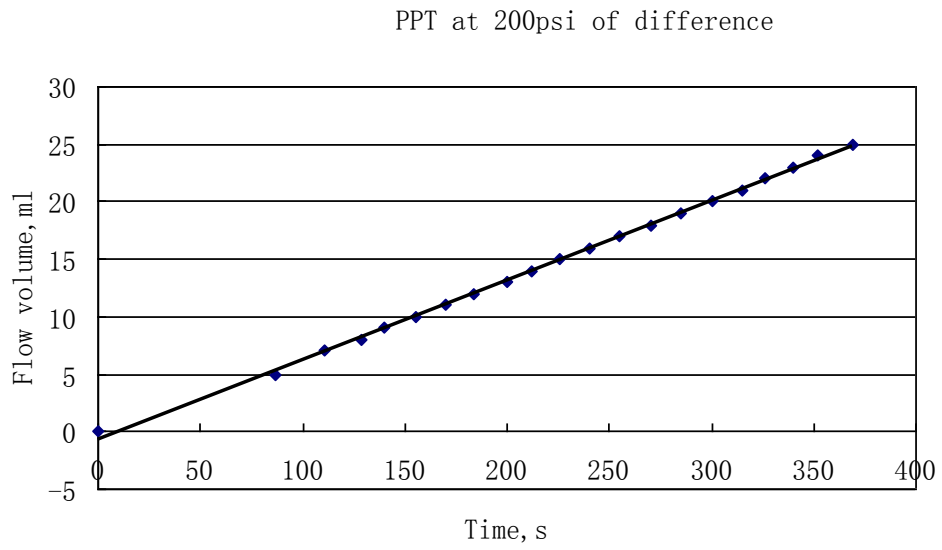

Figure 4.18 Darcy Flow Test with TGS

The resulting permeability is 281999 nD using the typical Darcy permeability equation. Figure 4.20 shows the second Darcy test keeping the upstream pressure to 100 psi and again measuring flow rate and calculating permeability.

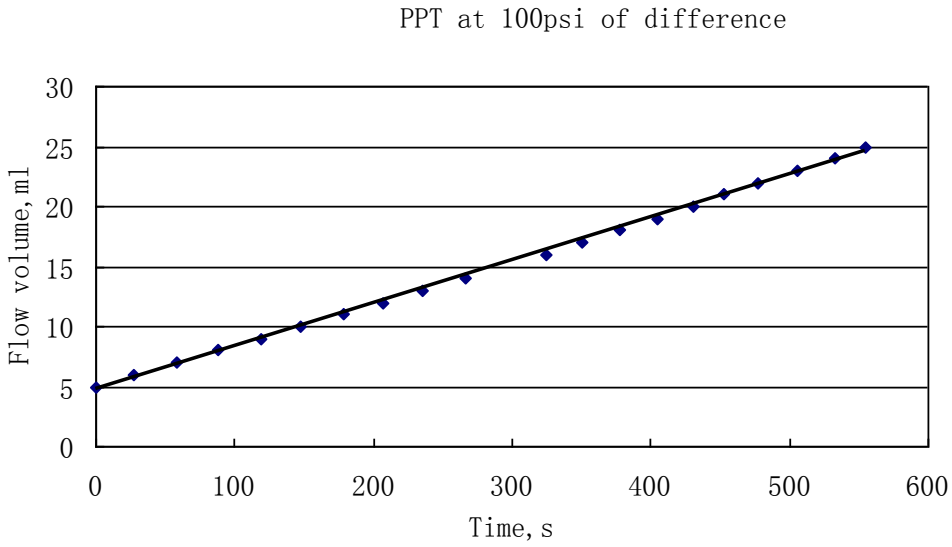

Figure 4.19 Darcy Flow Test with TGS

The resulting permeability from this test is 290964 nD (0.29 mD), and thus confirms the results from the first Darcy test. A permeability this high can only mean that the shale is cracked, observing that the permeability is almost in the milli-Darcy range. To see if the mud could plug this crack we followed the Darcy flow tests with the second step of the original test using a water-based mud. Figure 4.21 shows these results.

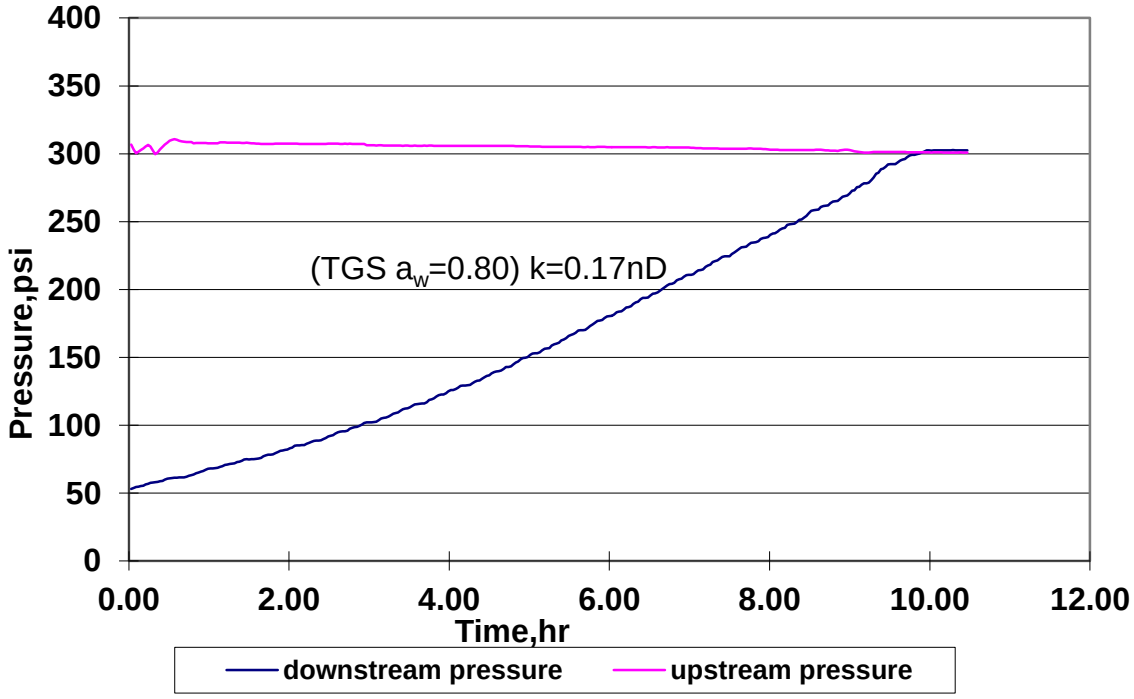

Figure 4.20 TGS with Water-based Mud

Even though the assumption that the shale is cracked, a very smooth curve is generated from this step. The smooth curve and low permeability of this step indicates that the water-based mud created a plug in the fracture or crack in the shale, and thus a normal permeability measurement can be assumed. The subsequent test confirms the

assumption that the shale crack is plugged by the mud particles. Figure 4.20, below, shows the result of the same mud with 10 ppb of NP's added as the injection fluid.

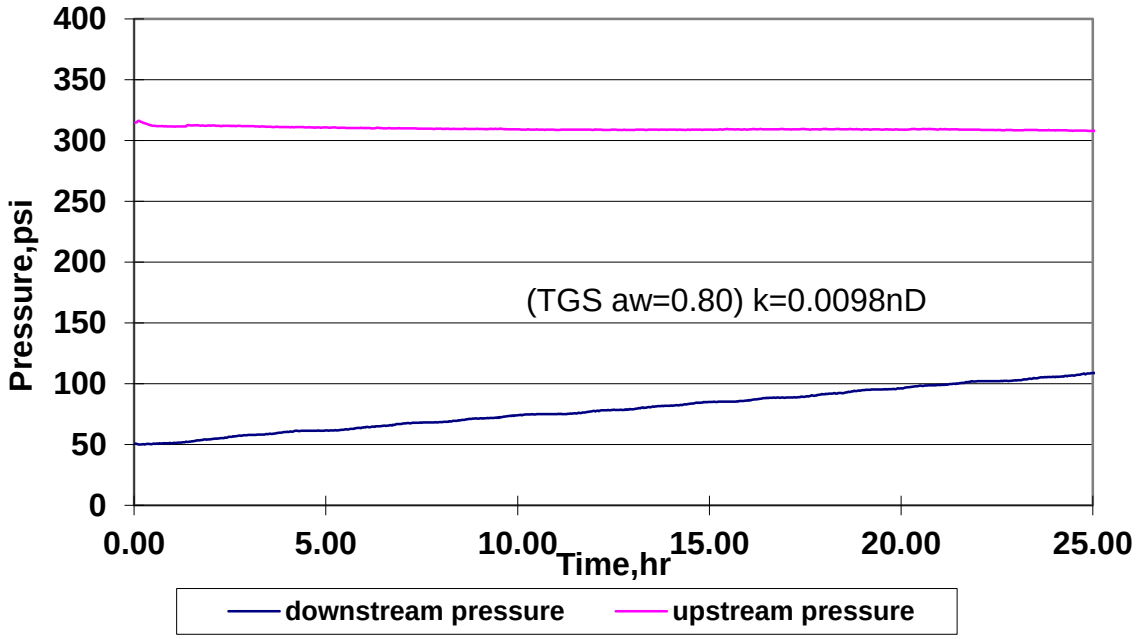

Figure 4.21 TGS with 10 ppb NP Water-based Mud

Comparing the three steps is vital to understanding what is occurring during the test. Figure 4.21, shown below, displays each step on the same time scale for comparison. In Figure 4.21 below, the permeability labeled "1. k = 0.073 nD" refers to the permeability before the shale cracks. The permeability after the crack is labeled with "2. k = 19.0 nD." The downstream pressure of the seawater step rapidly jumps indicating there is a crack at around 7 hours. After the initial seawater step was run, a Darcy type flow experiment was performed. The mud test, when compared to the seawater test, only partially plugged the crack in the TGS sample due to its permeability being higher than

the permeability of the sample before it cracked. The last step of the test using the NP's in the mud seemed to seal off the crack quite well. The resulting permeability from the NP mud is almost a whole order of magnitude lower than the original seawater test, even with the crack. The lower permeability also indicates that the NP's are actually plugging the pores of the shale.

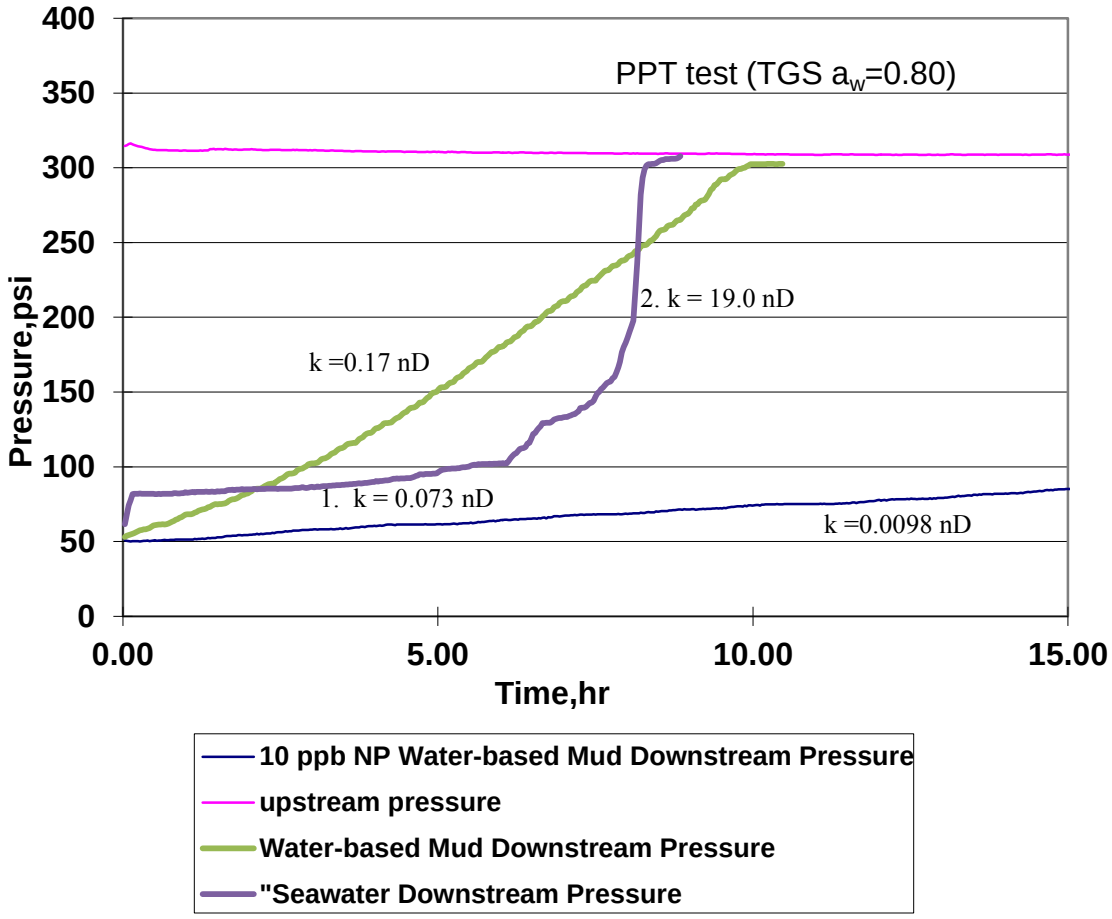

Figure 4.22 Three Step Mud Test with 10 ppb NP Mud

After this test was over, a physical analysis of the shale sample was made. The sample was removed from the Shale Test Cell and cleaned. The surface was then photographed, Figure 4.22 displays cracks in the shale sample.

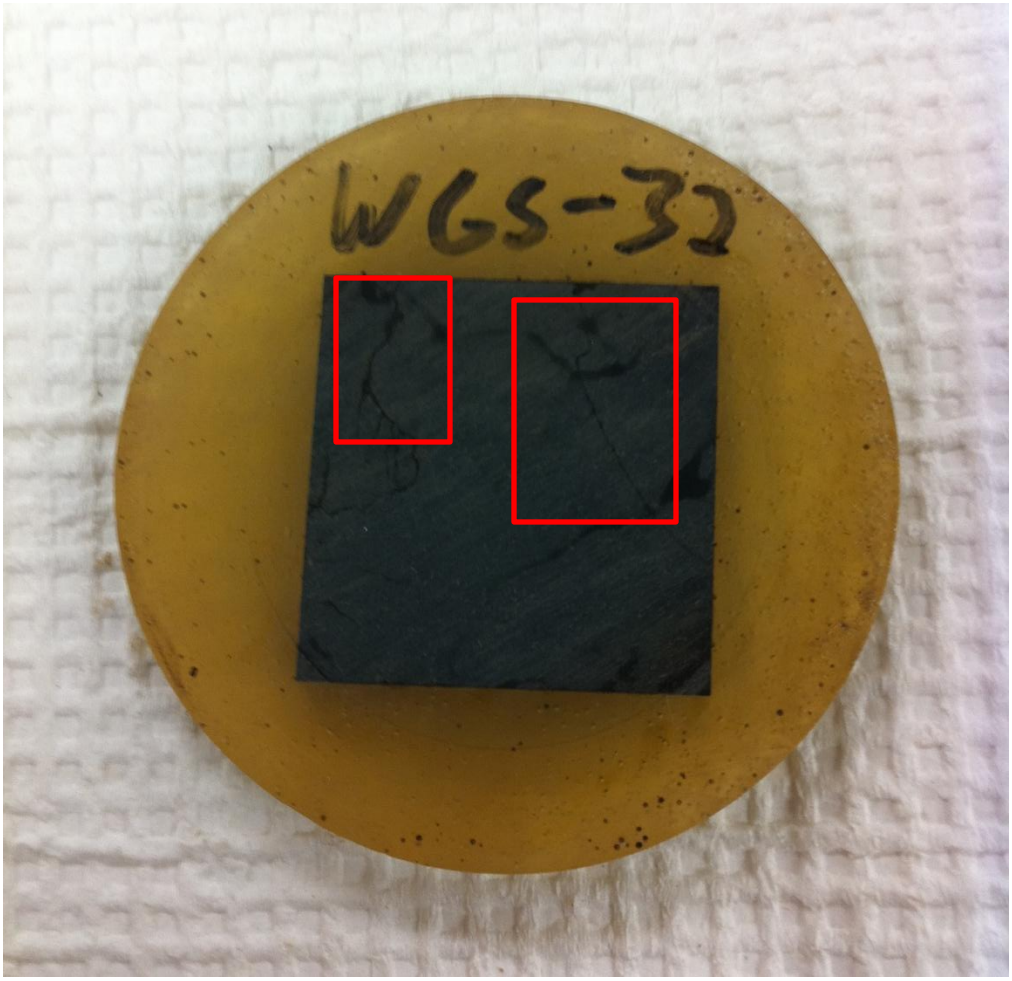

Figure 4.23 Cracked TGS Sample

Looking closely at Figure 4.22, the dark lines inside the red boxes on the shale surface are a result of fluid escaping the cracks in the sample. The surface was wiped clean and then washed with hexane to remove any residue from the mud. The picture was then taken, if too long of a period elapses before a picture is taken the fluid from the

cracks will dry up and makes the cracks much more difficult to see. Figure 4.23, below, shows the sample before it was washed as well as a bird's eye view of the cell with a brass ring on top of the sample to allow a gap for mud to flow across the surface.

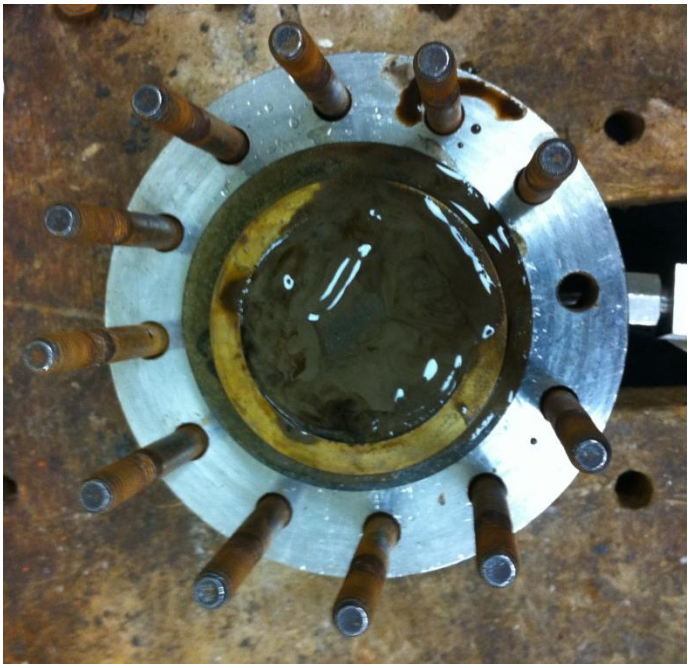

Figure 4.24 Unwashed TGS Sample with Mud in the Shale Test Cell

4.3 Foam Stability Test Results

After making enough foam to fill the 1000 mL accumulator, the previously mentioned stability tests were run on the foam with the different concentrations of NP's added. Table 4.1 tabulates the time it took for the foam to break down at atmospheric pressure.

NP Concentration (wt %)	Phase Separation (min)
0%	75
1%	94
2%	130
5%	123

Table 4.1 Phase Separation Time

Chapter 5: Discussion

5.1 Atoka Foam

Quantitative analysis of the permeability results is easier shown using graphical displays. Table 5.1 tabulates the permeability measurements from each test using Atoka Shale.

5% by wt. NP k (nD)			2% by wt. NP k (nD)			1% by wt. NP k (nD)		
Tapwater	Foam	NP Foam	Tapwater	Foam	NP Foam	Seawater	Foam	NP Foam
65.67	0.0887	0.00214	4.88	0.907	0.0215	12.5	0.0489	0.00824

Table 5.1 Permeability Results from Pressure Penetration Tests with Atoka

The color coding used in Table 5.1 is correlated to the shale sample used and is consistent throughout Chapter 5. In order to compare samples, Figures 5.1, 5.2, and 5.3 displays the water, foam, and NP foam permeability measurements respectively.

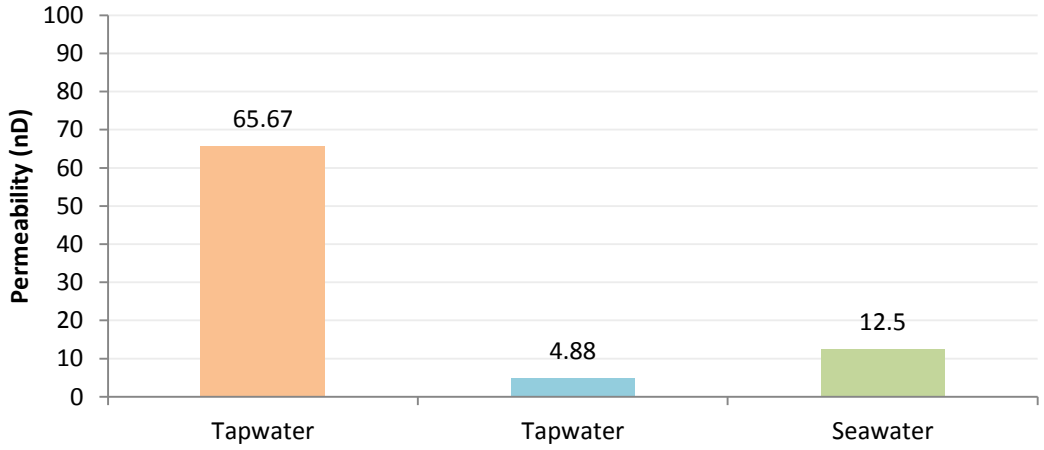

Figure 5.1 Water Permeability (nD) Bar Graph

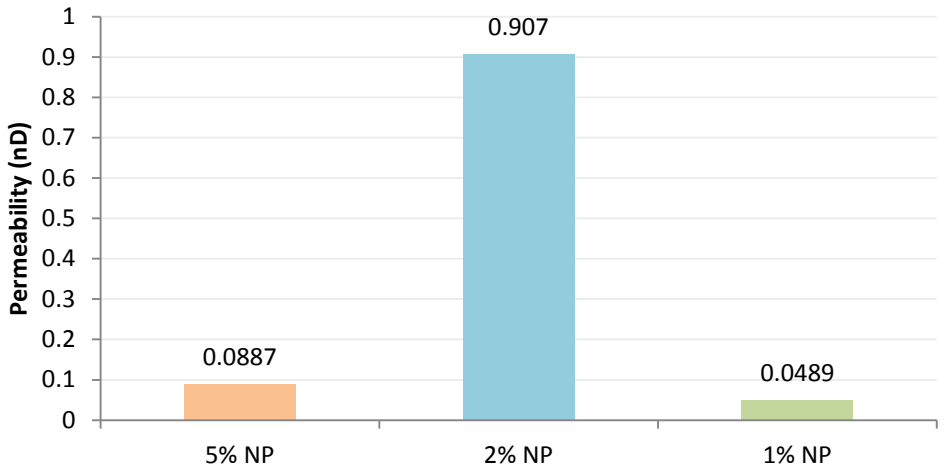

Figure 5.2 Foam Permeability (nD) Bar Graph

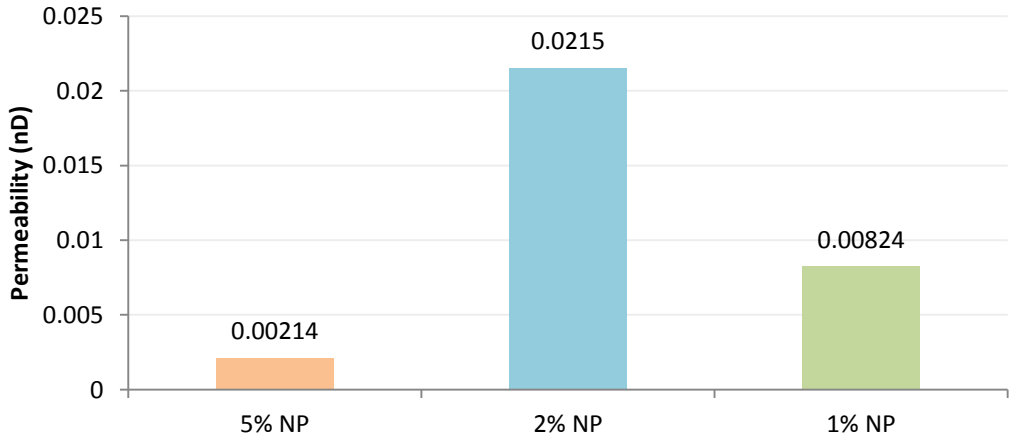

Figure 5.3 NP Foam Permeability (nD) Bar Graph

Figure 5.1 and 5.2 show the range of permeability between samples using the same fluids. Figure 5.4 below indicates the reduction of permeability from the water step to the initial foam without NP's step for each sample run. The 2% NP sample has a lower permeability reduction that the other two samples.

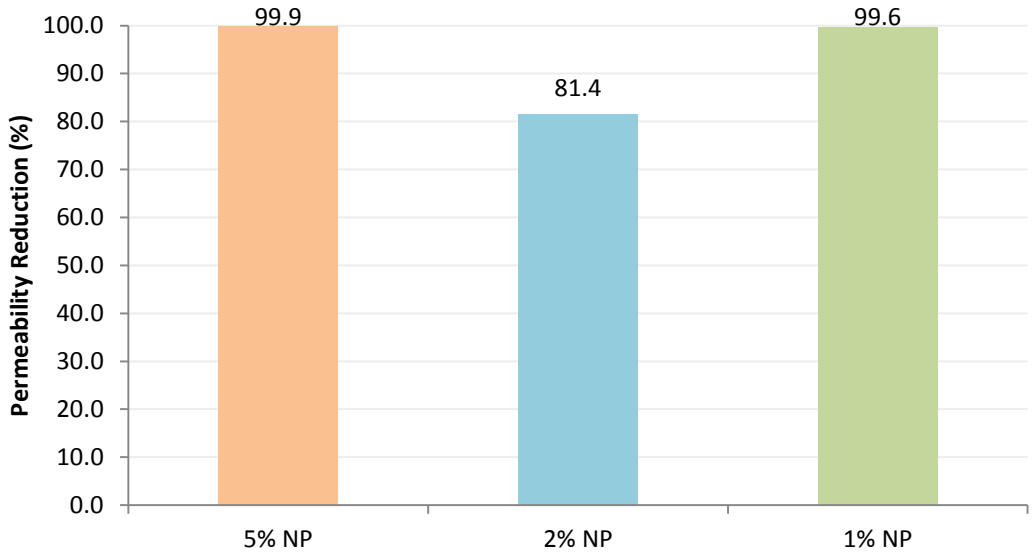

Figure 5.4 Water to Foam Permeability Reduction (%) Bar Graph

The lower permeability reduction could possibly be due to a micro-fracture in the sample that had widened sufficiently to allow foam to pass through the sample. It also could be just a natural phenomenon in variability in the shale sample.

With the assumption that nitrogen cannot enter the pores of the shale and that water can, permeability is reduced by the physical exclusion of water from the shale surface by nitrogen due to 70% of the volume of foam being nitrogen. With 70% of that area of the shale not contacting water, a 70% reduction of permeability would be expected as there is a direct correlation between permeability and area contacted. However, these results display an even further reduction in permeability. The surfactant enhanced liquid phase of the foam reduces surface tension between the nitrogen and the liquid film. The reduction in surface tension stabilizes the bubble surface and decreases the break down rate of the foam. When contacting the stable foam with the shale surface,

the foam bubbles do not readily break down, thus further limiting the amount of liquid available to flow into the shale. This mechanism of foam stability is likely the cause for the greater than 70% reduction in permeability.

Figure 5.5, shown below displays the reduction between the foam and foam with NP's.

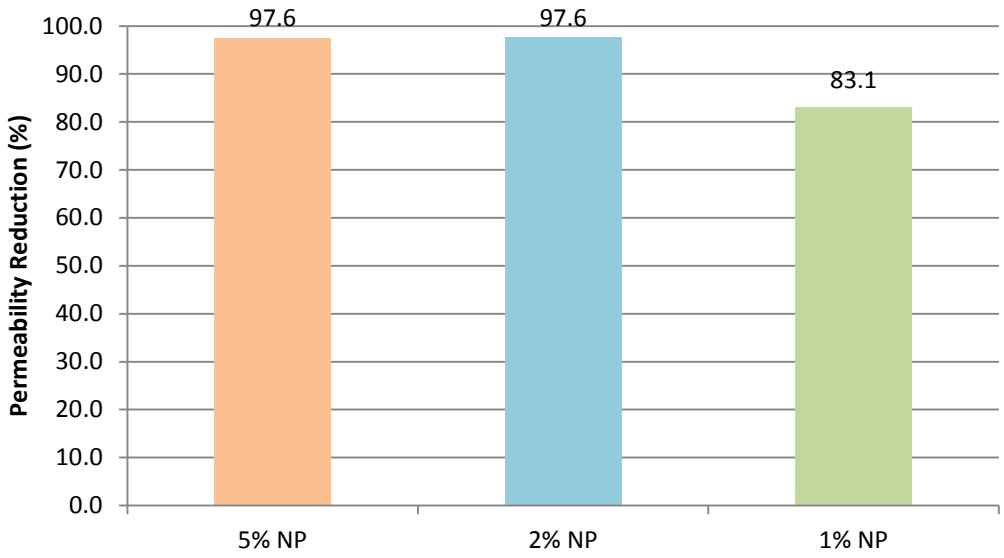

Figure 5.5 Foam to NP Foam Permeability Reduction (%) Bar Graph

Figure 5.5 suggests that a critical concentration of NP's added to foam exists. At 1% NP's added, the permeability reduction of the foam with NP's decreased to 83.1%. This may also be a natural phenomenon of the shale sample; further testing is needed to solidify this theory.

5.2 TGS ANALYSIS

Unsure whether the NP's would plug the pore throats of the TGS, a three step mud test and two "Darcy flow" tests were performed on the TGS. The permeability measurements are tabulated in Table 5.2, shown below.

Step	Test	Injection Fluid	k (nD)
1a	PPT	Seawater	0.073
1b	PPT	Seawater	19
2	DP =200 psi Darcy	Seawater	281999
3	DP =100 psi Darcy	Seawater	290964
4	PPT	Water-based Mud	0.17
5	PPT	10 ppb Water-based Mud	0.0098

Table 5.2 TGS with Water-based Mud (a denotes before crack, b denotes after crack)

The permeability measurements in steps 1-3 above indicate that the shale sample cracked, and the crack was then further widened by the two "Darcy flow" tests due to the high flow rate of fluid through the crack. After the "Darcy flow" tests, a Pressure Penetration Test was run using a WBM. The permeability measurement of 0.017 nD from this test suggests that the mud partially plugged the crack in the shale because it is lower than the 19.0 nD recorded in the shale sample using seawater after the crack was formed. After the normal WBM test was performed, the same Pressure Penetration Test was performed using the same mud with the addition of 10 ppb of NP's. The permeability measurement of 0.0098 from this test is a whole order of magnitude smaller than both the normal WBM test as well as the seawater test before the crack formed. This reduction in permeability suggests that the crack was successfully sealed as well as NP's were plugging the pore throats of the shale. This is a very important assumption because it validates the possibility of the TGS being plugged by the NP's.

The major difficulty using this TGS is the ease with which the samples crack. Unlike using mud, foam has no larger solid particles to plug a crack. Many samples were tested, of which only one sample suggested that the shale had no cracks of fractures. Table 5.3 below tabulates the permeability measurements from the one successful TGS sample.

TGS 2% by wt. NP		
Seawater	Foam	NP Foam
2.5	0.056	0.0013

Table 5.3 Permeability Results from Pressure Penetration Tests with TGS

These results receive validity when compared to the Atoka results discussed previously. Figures 5.6 and 5.7, below, shows the permeability reductions compared with the Atoka results.

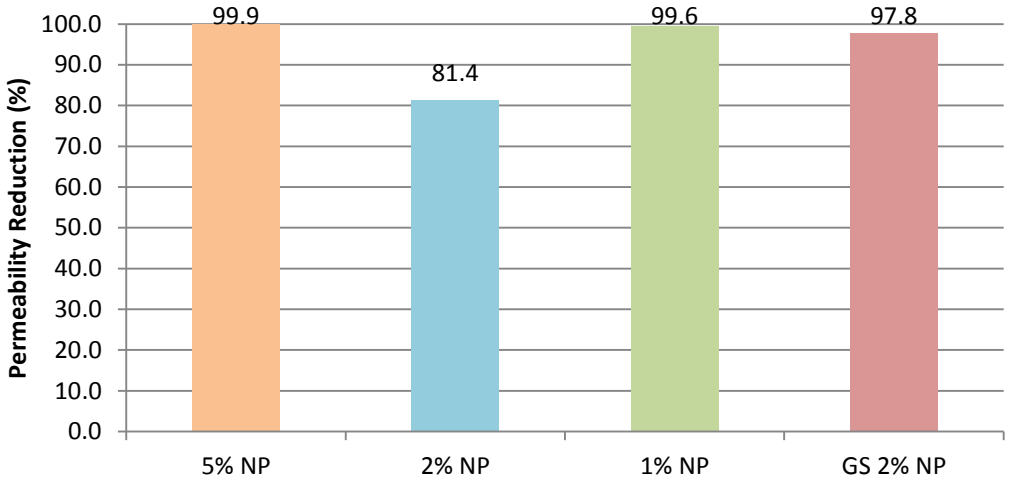

Figure 5.6 Water to Foam Permeability Reduction with Both Shale Cores

(GS denotes TGS)

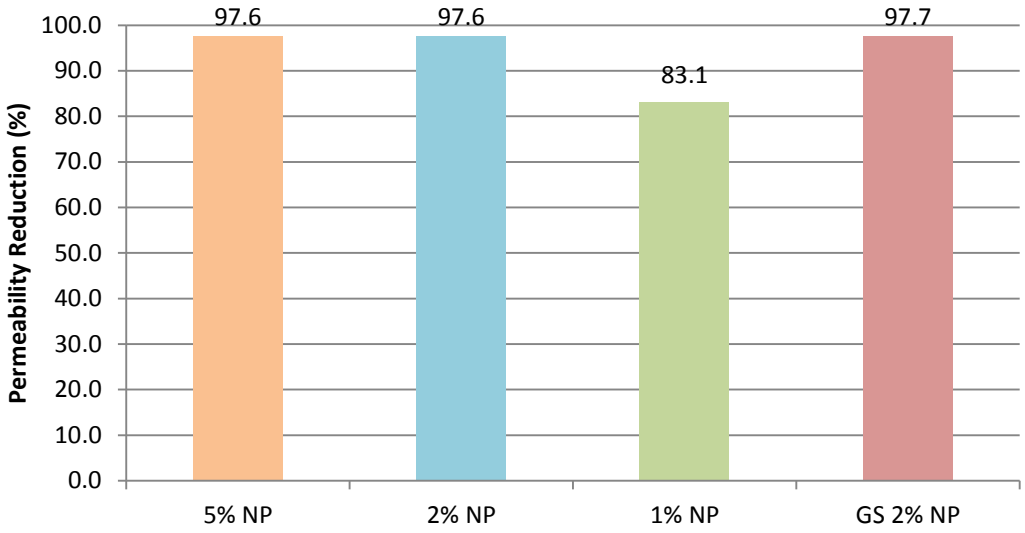

Figure 5.7 Foam to NP Foam Permeability Reduction (%) with Both Shale Cores (GS denotes TGS)

Figures 5.6 and 5.7 indicate that the results with the TGS sample are consistent with the Atoka Shale results. Further confirmation that the shale pore-throats were being plugged by NP's was uncovered as the sample of TGS was removed from the Shale Test Cell. Figure 5.8, shown below, has a high gloss coating on the surface of the shale sample. No other chemicals were added to the liquid phase of the foam besides surfactant and NP's. Process of elimination suggests that the sheen displayed below is a layer of NP's aggregating on the shale surface.

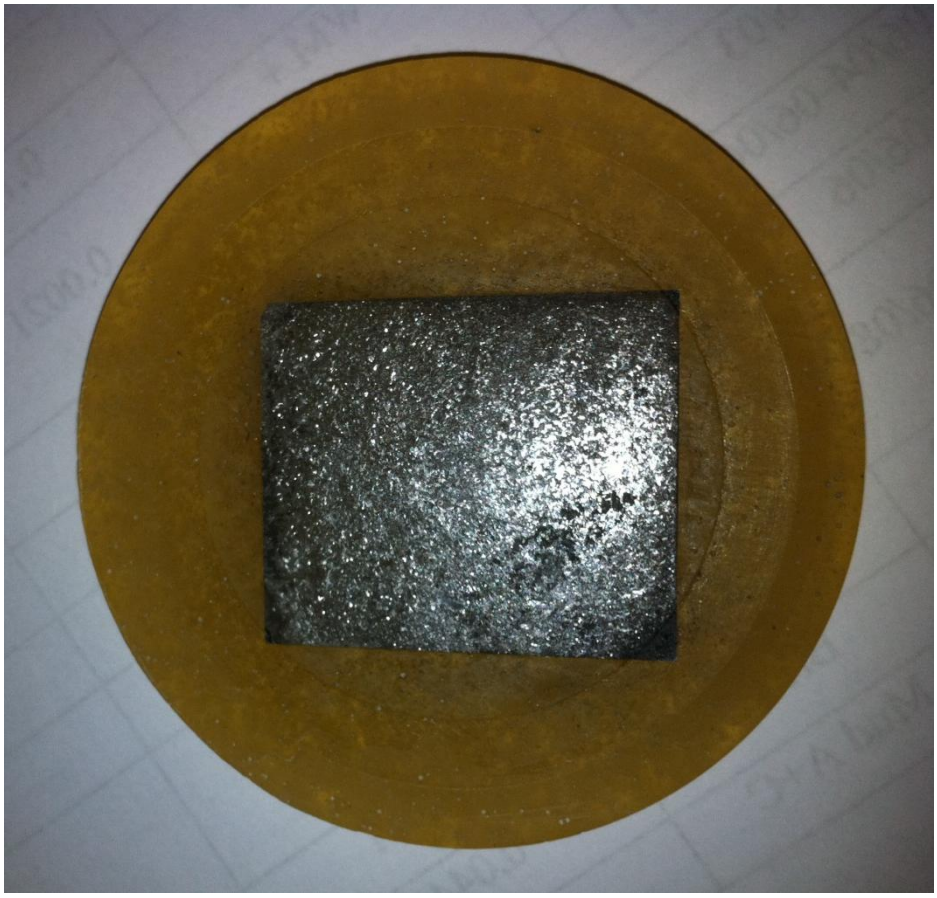

Figure 5.8 Upstream Side of TGS Sample After Three Step 2% NP Foam Test

In order to compare with the original sample appearance the opposite side of the shale sample is shown below in Figure 5.9.

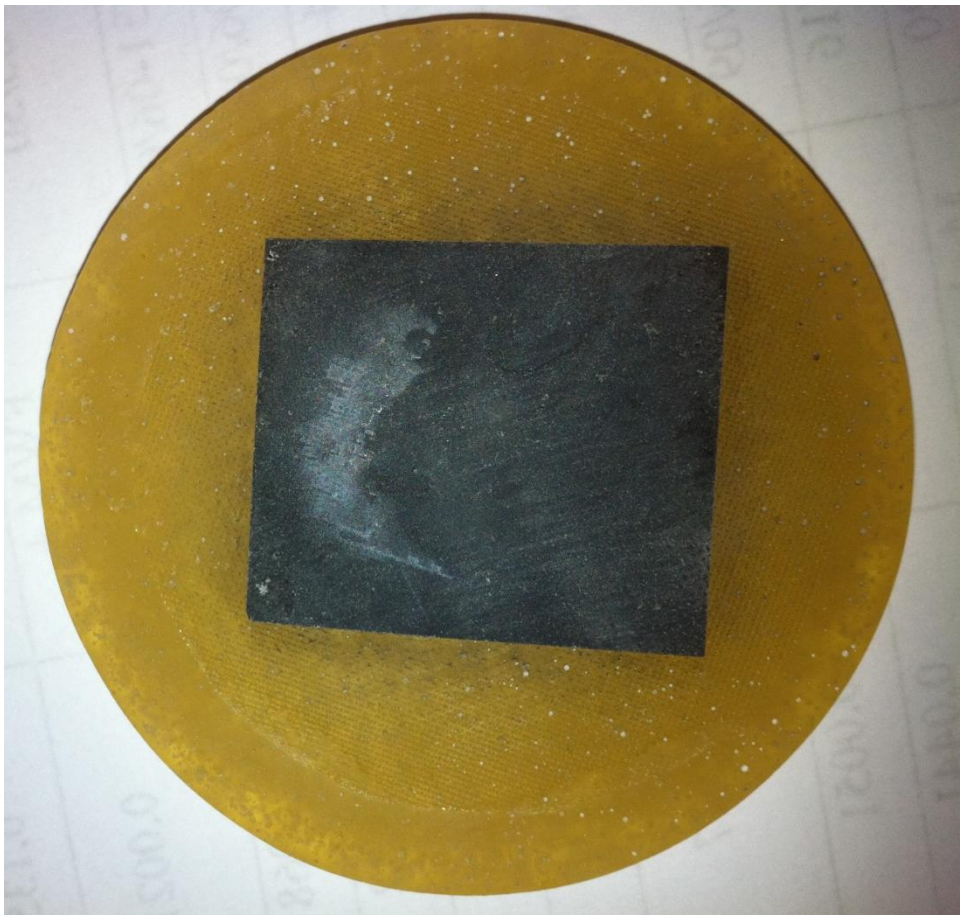

Figure 5.9 Downstream Side of TGS Sample After Three Step 2% NP Foam Test

From these results, it appears that the NP's are indeed plugging the shale pore-throats and partially responsible for the reduction in permeability between the foam and NP foam steps. Further testing of TGS needs to be completed for continued validation of these results.

An analysis of the TGS cracking and micro-fracture tendency can be found in Appendix A.

5.3 FOAM STABILITY ANALYSIS

When using foam in the field, mud pits may not have the capacity to hold the volume of foam needed to fracture or drill a well. The volume of gas increases as it exits the wellbore due to a reduction in pressure. Standard practice is to break the foam down on the rig floor so the liquid phase of the foam can be reused. To analyze the impact of the addition of NP's on breaking foam down at the rig floor under atmospheric conditions, several "table top" tests were performed to measure the time it takes for the foam to fully separate into separate phases. The results displayed in Table 4.1 are displayed graphically in Figure 5.10, shown below, to better understand the effect NP's have on foam stability at atmospheric pressure.

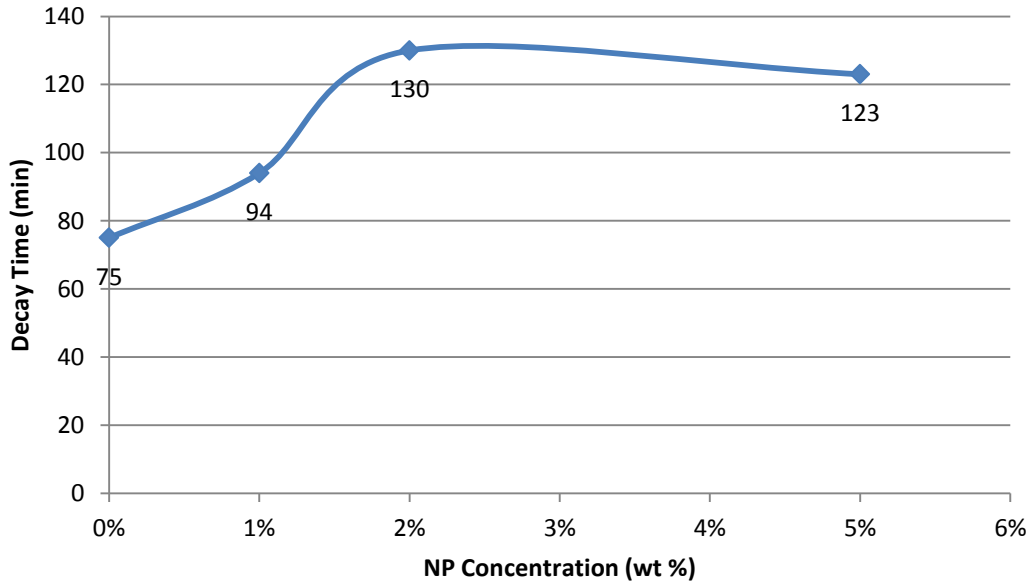

Figure 5.10 Foam Decay vs NP Concentration

The "Foam Decay" time is the time it took for the phases to completely separate. Figure 5.10 above suggests that a maximum NP concentration exists where increase of additional NP's to the foam decreases the stability of the foam. The extra weight of the NP's as concentration is increased, increases the force of gravity on the bubble surfaces causing an increased rate of drainage for the liquid phase.

The "Pickering Emulsion," discussed in Section 2.1, predicts an increase in stability of the foam with the addition of solid particles. The increase in stability by adding NP's to the foam is confirmed in Figure 5.10 by comparing the Decay Time between the foam without the addition of NP's to the 2% addition of NP's. The addition of 2% NP's doubled the Decay Time of the foam. The main concern at the rig floor is the power of the de-foaming agents normally used to break down the foam. Are these de-foaming agents strong enough to break down foam with NP's as well? Further testing is needed to investigate this issue.

5.4 Discussion of Foam with NP's Effect on Shale Permeability

Reviewing all the data presented above, two simultaneous mechanisms are proposed for the reduction in permeability of the shale due to the addition of NP's to the foam. Espinosa et al. (2010) have suggested at pressure, supercritical CO_2 and water foams are created and stabilized by NP's, even at very low concentrations. This idea has been borrowed to help explain the results shown above. Stability is indicated by the stability tests and the reduction of permeability between normal foam and NP enhanced foam. The increased stability of the foam due to the addition of NP's decreases the amount of liquid contacting the shale surface by adding resistance to the breaking of the

bubbles in the foam. Similarly to the surfactant used as the foaming agent, the NP's enhance the exclusion of water contacting the shale surface by forming stable bubbles in the foam. The bubbles cannot enter the pore throats due to the higher entrance pressure of nitrogen into the pores of the shale.

The second suggested mechanism for the reduction of permeability for NP enhanced foam is the plugging of pores by the NP's in the liquid phase of the foam. The liquid that does enter the pore throats contains NP's and has been shown in water-based muds by Sensoy et. al (2009) to plug the pore throats of the shale. The physical blocking of the pore throats restricts the flow of water into the pores of the shale. What is unknown about these two mechanisms is the extent of which each mechanism contributes to the reduction of permeability. The effects are seen simultaneously and the separation of each mechanism is difficult to explain, predict, and/or differentiate. Further testing is needed to investigate the contribution of each mechanism in the reduction of permeability in shale.

Chapter 6: Conclusions and Future Work

6.1 Conclusions

This study presents a set of results that shows that the addition of NP's to foam based drilling and fracturing fluids improves the performance of these fluids by reducing their invasion into shales. The following are specific conclusions can be arrived at based on the research presented.

- The addition of NP's to the liquid phase of foam physically plugs the pore throats of Atoka shale and TGS. The permeability of the shale was reduced by 83% to 97%. This feature makes this technology applicable to both drilling and fracturing operations.
- The addition of NP's in the liquid phase of foams stabilizes the foam by the creation of a "Pickering Emulsion."
- The use of foams reduces the amount of NP's needed in drilling of fracturing applications, making this technology much more economically feasible for field testing and use.

6.2 Future Work

The results present in this thesis clearly show that the use of NP's can improve the performance of drilling and fracturing fluids. However, a lot more testing and evaluation needs to be done in the future. Some specific suggestions for future work are presented below.

- Additional testing to validate the results of this study other shale samples.
- Additional testing of differing NP concentrations in foams on gas shale samples.

- Additional testing of differing NP concentration of foams for stability effects, both at atmospheric and higher pressure.
- Testing of defoaming agents on NP enhanced foams.
- Study of rheological effects from the addition of NP's in foam.

Appendix A

A.1 TGS Cracking and Micro-fracture Analysis

Testing this TGS core was more difficult than expected. The shale samples easily cracked or consisted of micro-fractures before testing was performed on the samples. Unlike Atoka Shale, TGS is a reservoir rock with significantly higher pore pressure due to fluids taking up the pore space inside the shale. This may be the cause of the shale cracking or developing micro-fractures. When the core is removed from the ground it releases the pore pressure and the rock stresses are removed. The release of rock stresses and/or pore pressure from shale with high carbonate content is most likely a cause of fractures. Evidence that the shale is cracked can be seen in Figure A.1 shown below.

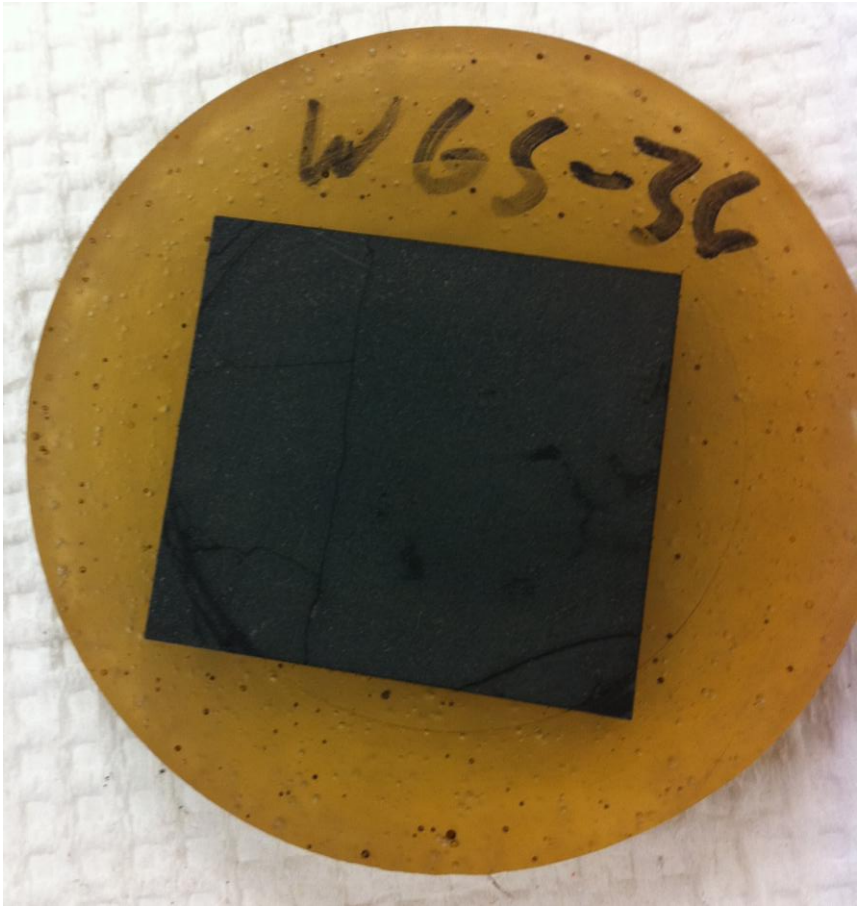

Figure A.1 Cracked TGS Sample

Tiny fractures and cracks can be seen in Figure A.1 above as the dark lines in the shale. Fluid exiting the cracks acts as a highlighter and makes it possible for the naked eye to see the fractures or cracks.

Another possible issue crossed while performing tests on samples that seem to be cracked is the shale to epoxy interface might have been leaking. After removing shale sample for the Shale Test Cell, many times cracks were not visible on the shale surface at all. Visible gaps have been seen on certain samples in past research, making it possible

for leaks across the shale epoxy interface possible. Since the TGS is a reservoir rock, oil can still occupy pore space. When the shale core is being prepared to enclose it with epoxy, an oil-wet saw is used to cut the core to the appropriate rectangular prism. Figure A.2, shown below, displays one of these rectangular prisms after the cutting process is finished.

Figure A.2 TGS Core Cut to Rectangular Prism

Figure A.2 shows the bedding planes of the shale core leaking out oil. In order for a proper seal between the epoxy and shale surface to form the oil must be washed off the surface with a solvent. Hexane was used to wash the surface of this shale sample repeatedly until very little oil came out of the bedding planes at all.

It is easy to see that certain sample cut ¼ of an inch in thickness could have a bedding plane that spans the height of the shale sample. These bedding planes then provide a conduit for fluid to pass through and show as cracks or fractures in the data generated.

After working with this TGS core, I would recommend the testing of a TGS core that has more quartz and sand content than high carbonate content. The carbonate content lends to the sample being very brittle and easily cracked. After the shale is cut to the desired shape and size, wash repeatedly with a solvent to free the surface of oil before encasing the shale in epoxy.

A.2 EQUIPMENT PICTURES

Below are some pictures of the equipment and setup used to perform the tests discussed above.

Figure A.3 Micropump Gear Circulatin Pump

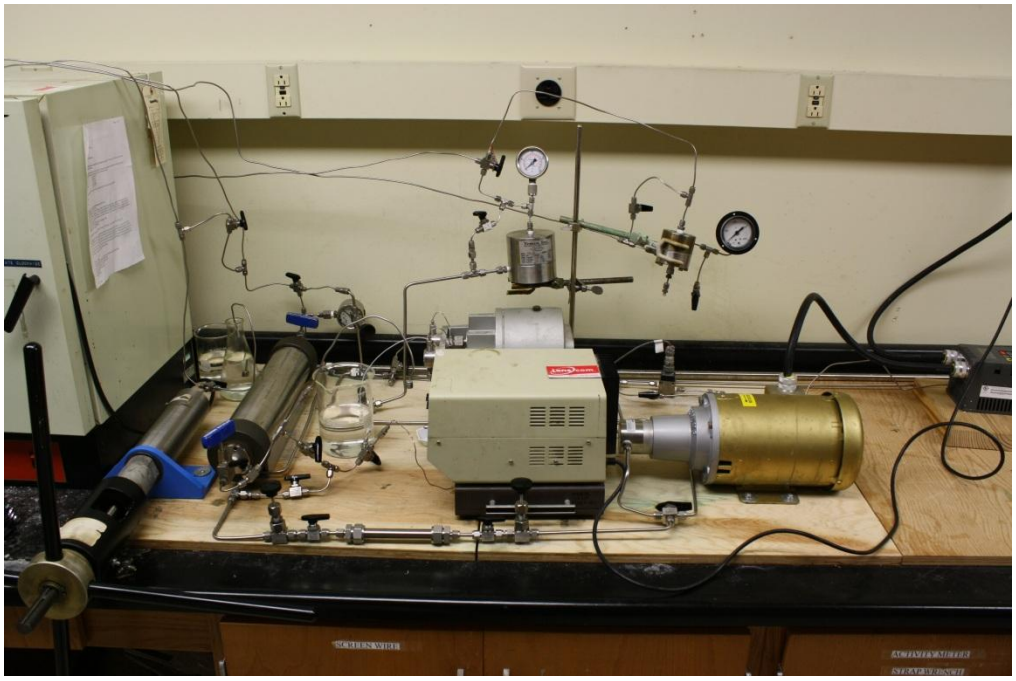

Figure A.4 Left Half of the Foam Loop

The liquid injection pump, circulation pump, both back pressure regulators, the manual pump, the accumulator, and density measuring device can all be seen in the above picture.

Figure A.5 Shale Test Cell and Pressure Transducers

Figure A.6 Close View of the Left Half of the Foam Loop

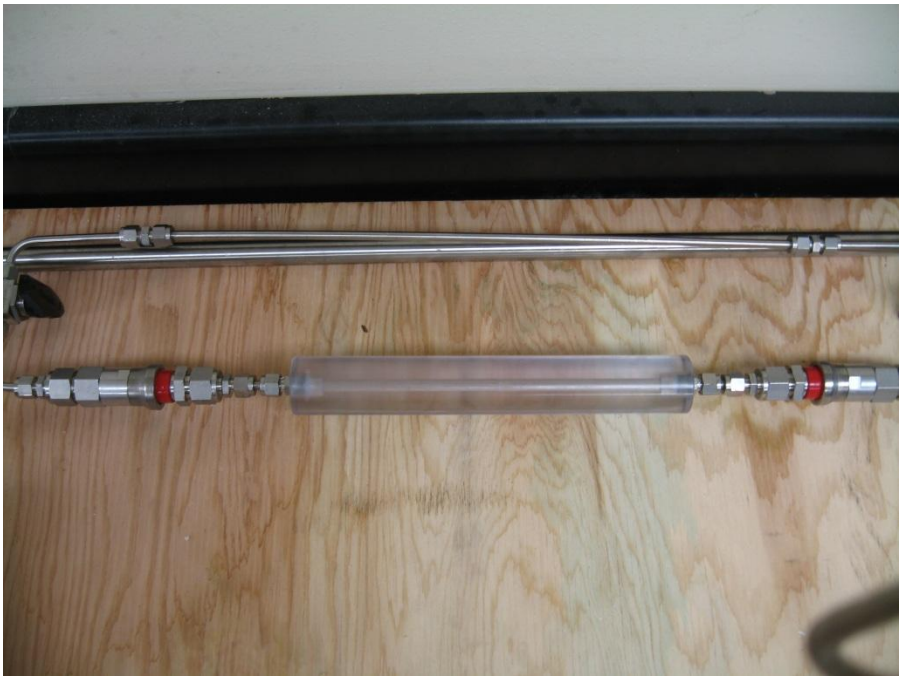

Figure A.7 Foam Viewing Cell with Quick Connects

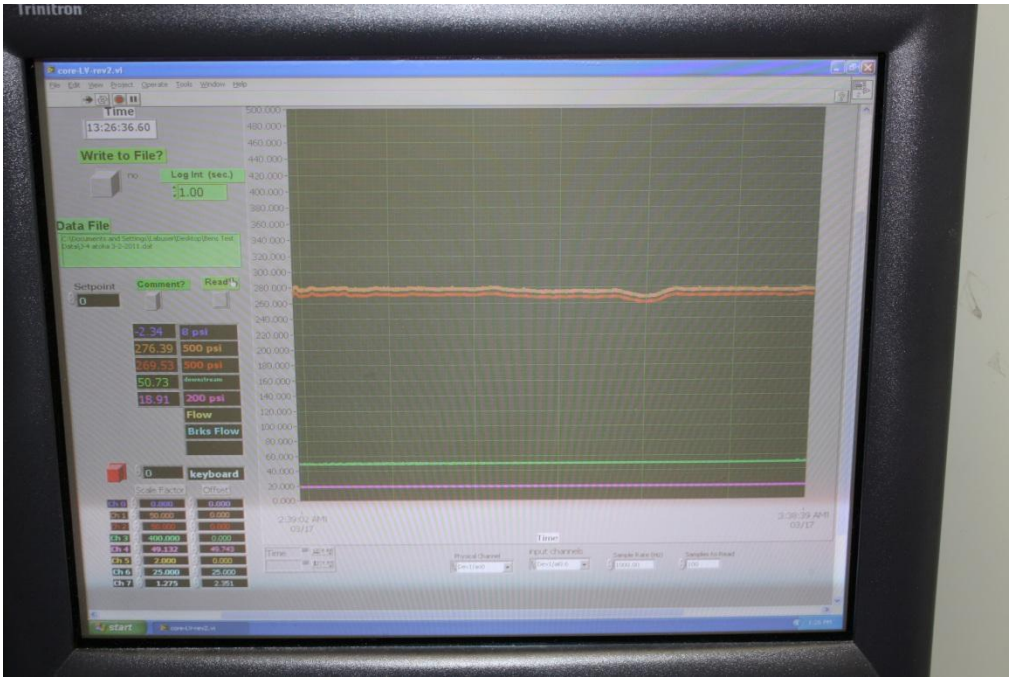

Figure A.8 Labview Software Gathering Data During a Test

Figure A.9 Close Up View of Foam Exiting the Outlet of Back Pressure Regulator

References

Abrams, A., 1977. "Mud Design to Minimize Rock Impairment Due to Particle Invasion." Journal of Petroleum Technology. May. 586-592

Al-Bazali, T. M., 2005 Experimental Study of the Membrane Behavior of Shale During Interaction with Water-base and Oil-Based Muds, Dissertation presented to the Faculty of the Graduate School of The University of Texas at Austin, Austin, Texas, USA, May

Al-Bazali, T. M., Jianguo Z., Chenevert, M. E., and Sharma M. M. 2009. An Experimentail Investigation on the Impact of Capillary Pressure, Diffusion Osmosis, and Chemical Osmosis on the Stability and Reservoir Hydrocarbon Capacity of Shales. Paper SPE 121451-MS was presented to the Offshore Europe SPE Conference, Aberdeen, UK, 8-11 September

Cawiezel, K.E. and Niles, T. D. 1987. Rheological Properties of Foam Fracturing Fluids Under Downhole Conditions. Paper SPE 16191 was presented at the SPE Hydrocarbon Economics and Evaluation Symposium, Dallas, Texas, USA, 2-3 March

Espinosa, D. Cladelas, F. Johnston, K. Bryant, S. L. Huh, C. 2010. Nanoparticle-Stabilized Supercritical CO_2 Foams for Potential Mobiliy Control Applications. Paper SPE 129925 was presented at the SPE Improved Oil Recovery Symposium, Tulsa, Oklahoma, USA, 24-28 April.

Hitchins, R.D and Miller J. M. 2003. A Circulating-Foam Loop for Evaluating Foam at Conditions of Use. This paper (SPE 80242) was first presented at the 2003 SPE International Symposium on Oilfield Chemistry, Houston, Texas, USA, 5–8 February.

McLennan, J., Carden, R. S., Curry, D., Stone, C. R., Wyman, R. E., 1997. *Underbalanced Drilling Manuel,* Chicago, Illinois: Gas Research Insitute.

Negrao, A.F. and Lage, A. C. V. M. 1997. An Overview of Air/Gas/Foam Drilling in Brazil. Paper SPE 37678 was presented at the SPE/IADC Drilling Conference, Amsterdam, The Netherlands, 4-6 March.

Paknejad, A. Schubert, J. Amani, M. 2009. Key Parameters in Foam Drilling Operations. Paper SPE 122207 was presented at the IADC/SPE Managed Pressure Drilling and Underbalanced Operations Conference and Exhibition, San Antonio, Texas, USA, 12-13 February.

Saintpere, S. Herzhaft, B. Toure, A. Jollet, S. 1999. Rheological Properties of Aqueous Foams for Underbalanced Drilling. Paper SPE 56633 was presented at the SPE Annual Technical Conference and Exhibition, Houston, Texas, 3-6 October.

Sensoy, T. Chenevert, M. E. Sharma, M. M. 2009. Minimizing Water Invasion in Shale Using Nanoparticles. Paper SPE 124429 was presented at the SPE Annual Technical Conference and Exhibition, New Orleans, Louisiana, USA, 4-7 October.

Suri A. and Sharma M. M. 2004. "Strategies for Sizing Paticles in Drilling and Completion Fluid." SPE Journal. March. 9:1:13-23

Tambe D.E. and Sharma, M. M. 1993. "Factors Controlling the Stability of Colloid-Stabilized Emulsions, 1. An Experimental Investigation," *J. Colloid and Interface Sci.* 157,244.

Wendorff, C. L. and Earl, R. B. 1983. Foam Fracturing Laboratory. Paper SPE 12025 was presented at the 58th Annual Technical Conference and Exhibition, San Francisco, California, USA, 5-8 October.DD